National and Kapodistrian University of Athens

Master's Thesis

Localization in Spatially Correlated Shadow-Fading Environment

Author:
George Arvanitakis

Supervisors:
Prof. Andreas Polydoros
Dr. Ioannis Dagres

Athens, 2014

Contents

List of Figures

List of Tables

Publications that this thesis created

1. Arvanitakis, George; Kaltenberger, Florian; Dagres, Ioannis; Polydoros, Andreas; Kliks, Adrian; "*Power-based localization in correlated log-normal fading aided by conditioning measurements*" EUCNC 2015, European Conference on Networks and Communications, June 29-July 2, 2015, Paris, France

2. Arvanitakis, George; Dagres, Ioannis;Kaltenberger, Florian; Polydoros, Andreas; "*Cramer Rao lower bound for multi-source localization in spatial correlated environment*" EUCNC 2015, European Conference on Networks and Communications, June 29-July 2, 2015, Paris, France

3. Arvanitakis, George; Dagres, Ioannis; Kliks, Adrian; Polydoros, Andreas; "*RSS based localization: Theory and experimentation*" EUCNC 2014, European Conference on Networks and Communications, Special session, From Theory to Practice: Experimental Research Activities in NEWCOM#'s EUWIN Labs, 26 June 2014, Bologna, Italy

Acknowledgements

"Communication in a foreign language is painful and feels as if half of me has disappeared". Manos Hatzidakis

As the Acknowledgements part is the most personal part of this document, I would prefer to present it in my native language.

Με την παρούσα διπλωματική εργασία κλείνει ένα σημαντικό κεφάλαιο της ζωής μου, αυτό των φοιτητικών μου χρόνων στο Φυσικό της Αθήνας (Προπτυχιακό και Μεταπτυχιακό).

Θα ήθελα να ευχαριστήσω αρκετούς ανθρώπους που αλληλεπίδρασα μαζί τους αυτά τα χρόνια και με καθόρισαν σε μικρό ή μεγάλο βαθμό.

Θα ξεκινήσω από τον Καθ. Ανδρέα Πολύδωρο που μου έδωσε την ευκαιρία να δουλέψω με τον ίδιο και την ομάδα του, όπου μαζί με τον Δρ. Ιωάννη Δαγρέ με καθοδήγησαν στα πρώτα μου ερευνητικά βήματα. Η καθοδήγηση αυτη, αν και θεωρώ τον εαυτό μου τυχερό που την είχε, ηταν ελάσσονος σημασίας συγκρινόμενη με το γεγονος ότι μου ανέδειξαν ένα μοντέλο ανθρώπου που μέχρι τότε αγνοούσα. Ενα μοντέλο το οποίο βρήκα γοητευτικό και πήρε με τη σειρά του κάποιο χώρο στην προσωπικότητά μου.

Επίσης, θα ήθελα να ευχαριστήσω τους φίλους και την οικογένεια μου. Αυτές τις δύο συνιστώσες που ποτέ δεν κατάφερα να τις διαχωρίσω πλήρως, καθώς, νοιώθω τους φίλους μου οικογένειά μου και την οικογένειά μου φίλους μου. Τους ευχαριστώ για την ανιδιοτέλεια και την αδιάκοπη στήριξη που μου παρείχαν όλα αυτά τα χρονιά.

Τέλος, να ευχαριστήσω από καρδιάς τα αστέρια, που φώτισαν μέσα στη νύχτα ώστε να μη χάσω τον δρόμο μου και μετά χαθήκανε.

Γιώργος Αρβανιτάκης

If burning your wings is the price to pay
to explore the boundaries, then this is the
dirty work that somebody has to do.
Thank you Icarus!

"Don Quixote's misfortune is not his
imagination, but Sancho Panza".

Franz Kafka

INTRODUCTION

Transmitter localization via distributed sensor networks is an enabling technology for a large set of applications. In particular, radio-source localization is viewed as an important element of upcoming cognitive radio networks [1]. Endowed with the capability to sense and process radio activity in the surrounding environment, cognitive radios can efficiently plan, decide upon, and execute their respective actions [2], [3].

In this thesis, sensing is based on simple received power. In radio jargon, this is called Received Signal Strength (RSS) and it is popular due to its simplicity as every radio measures power. The flip side of this simplicity is that RSS-based localization tends to be less accurate than competing, more complex schemes. This is because for RSS-based localization, deterministic power-law is not a reliable reception model. More advanced probabilistic (log-normal) propagation models include a shadow-fading random variable (rv) to describe the variation around the mean provided by the aforementioned power law. This is still not adequate, unless the spatial-correlation aspect of propagation is included in the model. Proper modeling information can be presumed available in modern networks endowed with databases, which extract the information from past or training measurements and offer it for future benefits.

This thesis experimentally examines the existence of spatial-correlation in the shadow-fading component. In addition, we are interested in a theoretical investigation of the gain achieved if we take into account the existence of shadow-fading spatial-correlation. As we will present in chapter 1, the knowledge of spatial-correlation modifies our optimization problem, from minimization of multi-variable independent Gaussians to a minimization of correlated joint-Gaussian distribution. Additionally, the thesis incorporates this spatial-correlation aspect and assesses its impact, in conjunction with the beneficial effect of prior training measurements. We adopt the term *conditioning measurements* (CM) to represent any such modeling enrichment or uncertainty reduction brought about by the availability of training, pilot-based information, past known results, or any other factor that will yield a conditional propagation density with better performance. Implicit in this conditioning is the existence of a sensor network that provided these, a network viewed as distinct from the one currently available used to collect the present measurements. For the sake of conciseness, the terms prior and current will be used to describe these two classes, although, in a general setting, time periods may not be the only qualifier of the information. A probabilistic (Bayes) interpretation of the respective terms yields a better understanding. In this work, we are interested in the simple single-source scenario as well as in the more challenging multi-source scenario.

Many models exist to describe spatial-correlation in shadow-fading environments [4]. Experiments have also been performed to measure it [5], [6], and various techniques have been proposed to take advantage of it in a solution [7]. Performance analysis and improvement of RSS-based localization in such an environment has been performed in [8], [9]. In [10], [11], the CRLB for Correlated Log-Normal (CLN) propagation was derived for different parameters.

We derive and present a new theoretical bound for the single-source localization problem that takes *spatial-correlation* as well as CM into account and then uses it to assess performance. One of the main benefits of such parametric performance quantification is the ability to address questions of network scaling. In particular, we can address questions such as: (1) What is the required density of RSS-based sensor networks (prior and current) for achieving a given localization accuracy? (2) How can current required density be reduced in light of the utilization of the prior network? (3) How are these two network densities (prior and current) related in general for a given propagation environment? Because the answers herein are based on rather simple analytical models for the propagation environment and the spatial statistics, another important question is (4) How close are these answers to the true performance typically seen in practice? This last question is difficult to answer, in general because any given trial represents a single realization of the underlying stochastic experiment. There have been qualitative arguments [8] on the value of exploiting spatial-correlation, but to provide hard, quantitative arguments there needs to be more extensive measurement campaigns.

Furthermore, we present some theoretical results in the more challenging multi-source localization problem again for the case of correlated shadow-fading environments. These results did not assume prior knowledge of conditional measurements, but show how the localization performance scales with respect to the number of sensors, the number of unknown sources, and the correlation coefficient of the environment. For the sake of completeness, these results should be extended also for the case of conditional measurements.

Two indoor experimental campaigns are included in this thesis, both of which used the OpenAirInterface (OAI) [12] platform. The main target of the campaigns was 1) to verify the existence of shadow-fading in the indoor environment and 2) to use ad-hoc techniques in our localization algorithms in order achieve some gain from spatial correlation assuming knowledge of conditional measurements.

The rest of this master's thesis is organized as follows: following the introduction, we present the state-of-the-art for the localization problem, mainly focusing on RSS techniques. Chapter 1 presents the CRLB propagation model. The statistics of RSS are derived with the inclusion of CM, since these are needed for the derivation of the CRLB. Furthermore, this CRLB is derived and is subsequently referred to in the semi-analytical performance assessment. In order to draw specific performance conclusions, two scenarios are selected, one indoor and one outdoor. Chapter 2 sets up and subsequently derives the CRLB for the multi-source problem, also assuming a spatially-correlated environment. This chapter provides an initial performance analysis regarding the number of sources, the number of sensors, and the de-correlation distance. Chapter 3 presents the first experimental campaign that aims at characterizing the shadow-fading. This campaign includes very dense measurements in order to capture the statistics of the shadow-fading. Subsequently, these results are used to examine the theoretical gain of different ad-hoc techniques. Finally, Chapter 4 shows the results of the second experimental campaign, which covers a wider area than the first, but the measurements are more sparse. Results of localization algorithms that used these measurements will also be presented.

State of the Art

RSS-based localization is not new [4], and it has been studied under various modeling assumptions, always in accordance with the specificities of the different applications at hand. The aspects in common of the related topics encourage a review of the proposed solutions on a broader scale than any one specific radio-based solution. For instance, there is a sizable body of work in the literature for energy-based localization of acoustic (i.e., non-radio) sources. The received-energy error-modeling assumption for such applications is typically Gaussian (i.e., additive Gaussian noise). This is not valid in the radio context and yet there are commonalities in the formulation of an algorithmic solution that are worth considering.

We review the SoA here from the standpoint of the different proposed methodologies, not from the standpoint of the target application. However, we will account for the modeling assumptions as they arise from the application.

To facilitate things, we first introduce some abbreviations. Among the many details that differentiate the modeling assumptions, the most important are: a) The number of active sources, in combination with the degree of time-frequency orthogonality for the case of more than one sources; and b) the mathematical model for the energy measurement. For (a), we will use the letter S for single source and M for multiple, followed by O whenever the sources are orthogonal in the measurement domain. The orthogonality assumption pertains to the nature of the measurement and not the type of application. If the energy of each source can be measured separately from the energy of others, then this is orthogonal modeling, whereas if the received energy is a superposition (sum) of all source energies, the model is non-orthogonal. For (b), we denote by L the log-normal propagation model, G for additive Gaussian noise, and I for indefinite modeling (in most cases, I pertains to a range estimate that is modeled as the true range plus Gaussian noise). So, for example, M-O-L stands for multiple sources, orthogonal measurements and log-normal propagation model.

We now move on to the categorization of the algorithmic design methodology. Here we can first identify two main categories which are in line with the modeling assumptions, namely the probabilistic and the non-probabilistic methods.

The non-probabilistic (geometric) methods either adopt an error-free measurement model or a very simple one. Although not primarily interested in this class, we review it since new hybrid methods can take advantage of it. The main challenge here is to derive the source location from the measurements, since the source location is related to the measurements in a highly nonlinear manner. The linearization of the measurement description model, the description of the noise under the selected model, and the algorithm for solving the resulted system of equations are the main tools of these solutions.

A measurement set or functions of multiple measurements are used to define a locus of possible source positions, and the intersection of the multiple loci defines the source position. Conventional approaches use measurement differences (either range or time), each one defining a hyperbolic line of position (LOP). The source position is found as the intersecting point of these hyperbolas [13], [14], [15]. In times past, this technique was viewed as computationally complex and not given to easy error analysis. An alternative method was proposed at [16], using a set of three sensors instead of two, resulting in straight instead of hyperbolic LOPs. This results in a convenient linear system of equations, but with a drawback of inconsistencies due to the use of redundant information. A afferent formulation was followed in [17], [18] that removed the redundancy, introducing however a non-linear term that required an inconvenient non-linear treatment (iterative gradient algorithms).This non-linearity was removed by a two-step procedure in [19], resulting in a closed-form expression for the source localization. These methods were proposed initially for TDOA measurements, but variations can be also used for RSS measurements. A similar but simpler method similar to [19] was proposed in [20] that allowed a performance prediction analysis. The modeling assumption was S-I. In [21], a constrained Weighted Least-Squares (WLS) approach was proposed for a RSS based S-G model, using again a quasi-linear description. This method was also applied for all types of measurements (TOA, TDOA, RSS, AOA) in [22]. In [23], a WLS-based, algebraic, closed-form solution was proposed again for S-G modeling, but now in 3-D space, and it proved that it reaches the CRLB (spell) when SNR (spell) tends to infinity. A similar approach was also provided in [24] for S-L modeling via TDOAs combined with gain ratios of arrival. A WLS approach that takes into account all error factors such as noise, shadowing plus modeling error in the path-loss exponent was proposed in [25] for S-L modeling. A BLUE (spell) plus an improved version was proposed in [26] by properly removing the bias that is introduced by the multiplicative shadowing noise (S-L). All such geometric methods have been formulated for the single-source case only. Multi-source cases have been proposed only for the case of M-O model assumption (see, for example, [27]).

Regarding the probabilistic category, Maximum Likelihood (ML) is the most popular estimation approach due to its asymptotic optimality. However, the likelihood function in a Gaussian or log-normal propagation environment typically possesses multiple minima, thus resulting in a non-convex optimization problem [28]; this, then, is the most significant drawback of the ML approach. Standard techniques for such non-convex optimization tend to be complex. In addition, computation increases exponentially with the number of sources. Various methods exist that try to maximize the likelihood function or approximations thereof. For multiple sources, research has mostly focused on the AWGN model, which is valid for acoustic sources. The same AWGN model has been applied to radio applications, but it turns out to be an oversimplification for log-normal shadowing environments.

We now review the SoA for this class. We define here as Direct these ML approaches that try to directly maximize the likelihood function (or approximations of it whenever its form cannot be precisely derived) by the use of any standard numerical technique. Usually performance bounds (such as the CRLB) are also derived whenever the pdf of the received measurements (parameterized by the position of the sources) can be obtained analytically. In [29] the authors consider source location estimation when the sensors can measure RSS (or TOA) between themselves and their neighboring sensors (M-

O-L modeling). The scenario assumes that a small fraction of sensors in the network have a known location (anchors), whereas the remaining sensor locations must be estimated. They derive the CRB and the maximum-likelihood estimators (MLE) under log-normal models (Gaussian for the TOA case). A distributed, RSS-based localization approach for S-L modeling is proposed in [30]. The approach also accounts for inaccurate range measurements by model fitting (calibration) from range measurements of known locations. A global optimization approach for RSS-based M-G model is followed in [31] using a particle swarm-based optimization technique. Spacel-based sensor clustering is also used to generate initial location estimates (single source estimation per sensor cluster), thereby increasing the likelihood that the particle-based optimizer reaches the global minimum. For the same model, a dominant-source based technique was proposed in [32]. The algorithm estimates iteratively the current dominant source, then removes its energy from the sensors, and continue in order to estimate the next dominant source. Heuristics are used for the clustering of the sensors that define the area of the dominant source. An approximate ML algorithm and associated performance bounds was proposed in [33] under S-L modeling for jointly estimating a transmitter' s position, orientation, beam-width, and transmit power, as well as the environment's path loss exponent, using RSS. A grid of possible positions is employed and for each point the ML estimates of the Tx power and the model parameters are computed. The space point with the maximum likelihood value is chosen as the estimate. In [34] an improved downhill simplex-genetic multiple source localization algorithm is proposed for M-G model. The only work that belongs in this category and which addresses the M-L model is [35], where a Gaussian approximation of the sum-log normal distribution is used for approximating analytically the likelihood function and simulated annealing is invoked to solve for the positions and powers of the sources. The unknown number of sources was treated by using a grid of possible source locations, while at the end, only the dominant sources are kept in heuristic fashion.

The next class includes approximate ML approaches. This is the most important category and includes: framework-based likelihood approximation such as Expectation Maximization (EM) or Space Alternating Generalized EM (SAGE); framework-based likelihood transformations or approximations such as convex feasibility or semi-definite programming (SDP) approaches. A Maximum Variance Unfolding (MVU) SDP-type algorithm for an M-O-I model was proposed in [36] along with upper and lower bounds on the reconstruction error.

The problem of local minima for an S-G model was addressed via projection on convex sets (POCS) in [28]. The algorithm is of low complexity, robust to local minima, and possesses a distributable computation. The distance estimates also employ RSS, but the algorithm can also be used for any positioning method where sensor-source distance estimates are somehow available. The method, named circular POCS, performs well when the (single) source node is located inside the sensor convex hull, defined by the outer perimeter nodes in the sensor network. When the Tx power of the source is unknown, measurements ratios are used instead. A diffusion-based distributed protocol for the same algorithm was provided in [37], [38] along with a theoretical analysis for each convergence.

Another method for addressing the non-convexity of conventional ML is the Semi-Definite Programming (SDP) relaxation technique mentioned above. The idea here is to convert the non-convex quadratic-distance constraints into linear constraints by introducing a relaxation that removes the quadratic term in the formulation. An SDP-based algorithm to initialize the ML minimization algorithm was proposed in [39], [40] for the S-L model which provides good performance by avoiding local minima. The same approach was followed in [41] for the S-G model. The extension of the method to M-O-L model was proposed in [42] for non-cooperative and cooperative schemes. An SDP approach for the S-L model with unknown source Tx power is given in [43] and extended for the M-O-L model in [44]. An EM-based algorithm for the S-L model was proposed in [45] treating the shadow-fading factors as the unobserved (missing) data. An EM-like method for M-G modeling was proposed in [46]. Classic EM approaches for the same model were proposed in [47], [48], [49]. The non-analytical nature of the pdf for the sum of log-normal variables does not allow a direct application of the EM framework. A quasi Expectation-Maximization (EM) method was proposed in [50], [51] by using the sum of log-power errors as a proxy objective function.

The aspect of the unknown number of sources was first addressed in [52], using a methodology called compressed sensing (CS) that exploits the inherent sparsity of the problem (small number of sources, large number of measurements). Under the M-G model, (recovery from noisy measurements) the Basis Pursuit Denoising (BPDN) [53] was employed along with a fixed point continuation method [54] to solve the BPDN optimization efficiently. In [55] they use Basis Pursuit (BP) [56], Basis Pursuit Denoising (BPDN), and Dantzig Selector (DS) [57] for $l1$-minimization programs, and compare their performance for location estimation in the M-L case. A pre-processing procedure on the original measured data is introduced to induce incoherence needed in the CS theory; and a post-processing procedure to compensate for the spatial discretization caused by the grid assumption. A cooperative splines-based spatial model approach was proposed in [58]. The model entails a basis expansion of the spectrum density (PSD) in frequency, weighted by unknown spatial functions that are estimated from power measurements. A novel model estimator is also developed using a least-squares (LS) criterion regularized with a smoothing penalty. The parameters of the model incorporate the information for the position of the sources. The framework fits better to an M-G model, but can be used also in M-L. A non-convex $l1$-regularized least squares scheme was also proposed in [59] for M-G. They decompose the difficult joint multi-source localization and environment perception problem into two simple sub-problems; one for multi-source localization and another is for environment perception. The two sub-problems were solved via the Gauss-Seidel [60], [61] technique and via the gradient descent algorithm with varying step-size, respectively. In [62] the authors continue their work in [58] and propose a distributed approach by suitably modifying the least-absolute shrinkage and selection operator (LASSO). The resulted novel cooperative sensing approach, named D-Lasso, was designed to be implemented in an ad-hoc network where the radios exchange information locally only with their one-hop neighbors, eliminating the need for a fusion (solution) center, and with claimed guaranteed convergence to the globally optimum solution. A low-complexity source location based on CS was proposed in [63].To speed up the algorithm, an effective construction of multi-resolution dictionary is introduced. Furthermore, to improve the capacity of resolving two sources that are close to each other, the adaptive dictionary refinement and the optimization of the redundant dictionary arrangement (RDA) are utilized [64], [65]. In [66], the authors argue that there is potential information within the cross-correlations of the received signals at different access points of a wireless network, which is not exploited in existing algorithms. To exploit this information, they proposed to construct a new fingerprinting map to include these cross-correlations and have shown that this new framework leads to obtaining an improved performance in terms of accuracy and number of localizable targets.

Chapter 1

Power-based localization in correlated log-normal fading aided by conditioning measurements

Parts of chapter 1 and chapter 3 included at: Arvanitakis, George; Kaltenberger, Florian; Dagres, Ioannis; Polydoros, Andreas; Kliks, Adrian; "*Power-based localization in correlated log-normal fading aided by conditioning measurements*" EUCNC 2015, European Conference on Networks and Communications, June 29-July 2, 2015, Paris, France

This chapter addresses the performance evaluation of power-based localization via the Crammer-Rao Lower Bound (CRLB) of a source in spatially-correlated log-normal propagation. The novel element is the inclusion and assessment of the impact of *conditioning measurements* on such performance. The proposed model parameterizes performance by both the sensor topology (density, positioning), resulting in the current measurements, as well as by CM (essentially, prior or training data), which reduces the statistical uncertainty in the model.

Propagation Model

RSS measurements are drawn either from a set of sensors in a prior network (which lead to CM) or from a current network. The current scenario assumes known sensor positions plus a single active emitter within an area of interest. This leads to three unknown parameters under estimation: two flat-plane coordinates plus the transmit power of the emitter.

We adopt the classic log-normal propagation model

$$R_i = P^{tx} - L_0 - 10\alpha log(d_i/d_0) + n_i^s + n_i^f \ , \tag{1.1}$$

where R_i is the source power, measured by i-th sensor or RSS, $d_i = \|\mathbf{x}_i - \mathbf{s}\|$ is their respective distance ($\mathbf{x}_i$,$\mathbf{s}$ are the coordinates of i-th sensor and source, respectively), P^{tx} is the emitter power, d_0 is a reference distance and L_0 is the power loss in that reference distance, α is the path-loss exponent, n_i^f is the noise due to fast-fading, which is hereby modeled as zero-mean Gaussian (in linear scale) and (n_i^s) is the shadow-fading rv. We follow common practice and reduce the effect of fast-fading by averaging measurements taken around the true location. This maybe seem unpractical (since we don't know where the source is), but the same effect can be had by moving the sensors around a bit instead of the source. It follows the above log-normal distribution: a Gaussian rv in the log domain with zero mean and variance σ_s^2.

Typical power model in log-normal fading

The typical model used does not account for CM, plus the sensors are considered far apart from each another, with zero spatial-correlation. Let $m_i(\theta) = P^{tx} - L_0 - 10\alpha log(d_i/d_0)$, then, for $\theta = [P^{tx}, L_0, d_0, \alpha, x, y]$ as the unknown parameters under estimation, we have

$$R_i = m_i(\theta) + n_i^s \ , \tag{1.2}$$

so, R_i follows Gaussian pdf

$$P_i(R_i|\theta) = \frac{1}{(\sigma_s\sqrt{2\pi})} e^{\frac{-\left(R_i - m_i(\theta)\right)^2}{2\sigma_s^2}} \ . \tag{1.3}$$

Due to zero spatial-correlation, the joint pdf becomes

$$P(\mathbf{R}|\theta) = \prod_{i=1}^{N} P_i(R_i|\theta) \ , \tag{1.4}$$

for the vector measurement $\mathbf{R} = [R_1, \cdots, R_N]$.

Power model in log-normal fading under CM

The propagation model is the same as above. In addition, let $R_i^{\{t\}}$ be the current measurement rv of the i-th sensor from the source at a location $\mathbf{t} = (x, y)$ and let $\mathbf{R}_i^{\{p\}}$ be the vector of M CM (say, derived from a training source and a prior sensor network) at locations $\mathbf{p} = [\mathbf{p}_1, \ldots, \mathbf{p}_M]$. The pdf for all measurements (in dB) is modeled as joint Gaussian:

$$\begin{bmatrix} R_i^{\{t\}} \\ \mathbf{R}_i^{\{p\}} \end{bmatrix} \sim N\left(\begin{bmatrix} \mu_i^{\{t\}} \\ \mu_i^{\{p\}} \end{bmatrix}, \begin{bmatrix} \sigma_i^{\{t\}} & \mathbf{C}_i^{\{t\times p\}} \\ \mathbf{C}_i^{\{p\times t\}} & \mathbf{C}_i^{\{p\}} \end{bmatrix}\right) \ , \tag{1.5}$$

where

$$\begin{aligned} \mu_i^{\{t\}} &= P_T - 10\alpha log(d_i^{\{t\}}) \\ \mu_i^{\{p\}} &= P_T - 10\alpha log(\mathbf{d}_p^{\{t\}}) \\ \sigma_i^{\{t\}} &= \sigma^2 \end{aligned} \ , \tag{1.6}$$

$$C_i^{\{p\}} = \sigma^2 \begin{bmatrix} \rho_i^{\{p_1\}} & \cdots & \rho_i^{\{p_1\times p_M\}} \\ \vdots & \ddots & \vdots \\ \rho_i^{\{p_M\times p_1\}} & \cdots & \rho_i^{\{p_M\}} \end{bmatrix} \ , \tag{1.7}$$

and

$$C_i^{\{p \times t\}} = C_i^{\{t \times p\}^T} = \sigma^2 \begin{bmatrix} \rho_i^{\{p_1 \times t\}} \\ \vdots \\ \rho_i^{\{p_M \times t\}} \end{bmatrix} . \tag{1.8}$$

Here, $P_T = P^{tx} - L_0 - 10\alpha log(d_0)$ is a simplifying parameter, which assumes that the source(s) providing the CM and the current source have the same transmit power. $d_i^{\{t\}}$ is the unknown distance between the emitter and the i-th sensor and $\mathbf{d}_i^{\{p\}}$ is $M \times 1$ vector with the known distances between the i-th sensor and the positions of the CM (totally we have M CM positions). Also, $\rho_i^{\{p_k \times p_j\}} = e^{-\alpha_c d^{\{p\}}}$ is the correlation factor and $d^{\{p\}}$ is the distance between p_k and p_j pilot transmitters. The correlation constant is depicted as α_c and the de-correlation distance is defined as $d_c = 1/\alpha_c$. It is also assumed that the standard deviation of the shadow-fading is equal for all sensors, i.e. $\sigma_i^{\{p\}} = \sigma$. Finally $\rho_i^{\{p_k \times t\}}$ is the correlation factor between the p_k pilot and the unknown transmitter.

Thus, the conditional pdf of $R_i^{\{t\}}$ given $\mathbf{R}_i^{\{p\}} = \mathbf{r}_i^{\{p\}}$ ($\mathbf{r}_i^{\{p\}}$ are the specific values of the CM) is also Gaussian $N\left(\mu_i^{\{t|p\}}, \sigma_i^{\{t|p\}^2}\right)$ with mean and variance given by

$$\begin{aligned} \mu_i^{\{t|p\}} &= E\left\{R_i^{\{t\}} | \mathbf{R}_i^{\{p\}} = \mathbf{r}_i^{\{p\}}\right\} \\ &= \mu_i^{\{t\}} - \mathbf{C}_i^{\{p \times t\}^T} \mathbf{C}_i^{\{p\}^{-1}} \left(\mu_i^{\{p\}} - \mathbf{r}_i^{\{p\}}\right) , \end{aligned} \tag{1.9}$$

and

$$\sigma_i^{\{t|p\}^2} = \sigma^2 - \mathbf{C}_i^{\{p \times t\}^T} \mathbf{C}_i^{\{p\}^{-1}} \mathbf{C}_i^{\{p \times t\}} . \tag{1.10}$$

Therefore $\mathbf{R}^{\{t\}} \sim N\left(\mu\left(\theta\right), \mathbf{C}_s\left(\theta\right)\right)$, where

$$\mu\left(\theta\right) = \left[\mu_1^{\{t|p\}}, \mu_2^{\{t|p\}}, \cdots, \mu_N^{\{t|p\}}\right] , \tag{1.11}$$

is the $N \times 1$ mean vector and

$$\mathbf{C}_s\left(\theta\right) = \begin{bmatrix} \sigma_1^{\{t|p\}^2} & \cdots & 0 \\ \vdots & \ddots & \vdots \\ 0 & \cdots & \sigma_N^{\{t|p\}^2} \end{bmatrix} , \tag{1.12}$$

is the $N \times N$ covariance matrix between the sensors, already calculated. Both depend on θ. In sum, the pdf of the received power is

$$\begin{aligned} P\left(\mathbf{R}^{\{t\}}; \theta\right) &= \frac{1}{(2\pi)^{\frac{N}{2}} \, det\left[\mathbf{C}_s\left(\theta\right)\right]^{\frac{1}{2}}} \\ &\exp\left[-\frac{1}{2}\left(\mathbf{R}^{\{t\}} - \mu\left(\theta\right)\right)^T \mathbf{C}_s^{-1}\left(\theta\right)\left(\mathbf{R}^{\{t\}} - \mu\right)\right] . \end{aligned} \tag{1.13}$$

Cramer-Rao Lower Bound

The Fisher information matrix for Gaussian rv is (see [67]):

$$\begin{aligned}[I(\theta)]_{kl} =& \frac{1}{2} tr\left(\mathbf{C}_s^{-1}(\theta)\frac{\partial \mathbf{C}_s(\theta)}{\partial \theta_k}\mathbf{C}_s^{-1}(\theta)\frac{\partial \mathbf{C}_s(\theta)}{\partial \theta_l}\right) \\ &+ \frac{\partial \mu(\theta)^T}{\partial \theta_k}\mathbf{C}_s^{-1}(\theta)\frac{\partial \mu(\theta)}{\partial \theta_l}\,,\end{aligned} \tag{1.14}$$

which $tr()$ is the trace of the matrix. We thus need to calculate the partial derivatives

$$\frac{\partial \mathbf{C}_s(\theta)}{\partial \theta_k} = \begin{bmatrix} \frac{\sigma_1^{\{t|p\}^2}}{\partial \theta_k} & \cdots & 0 \\ \vdots & \ddots & \vdots \\ 0 & \cdots & \frac{\sigma_N^{\{t|p\}^2}}{\partial \theta_k} \end{bmatrix}, \tag{1.15}$$

where

$$\begin{aligned}\frac{\sigma_i^{\{t|p\}^2}}{\partial \theta_k} =& -2\sigma_i^{\{t|p\}}\left[\frac{\partial C_i^{\{p\times t\}^T}}{\partial \theta_k} C_i^{\{p\}^{-1}} C_i^{\{p\times t\}}\right. \\ &\left. + C_i^{\{p\times t\}^T} C_i^{\{p\}^{-1}} \frac{\partial C_i^{\{p\times t\}}}{\partial \theta_k}\right],\end{aligned} \tag{1.16}$$

and

$$\frac{\partial C_i^{\{p\times t\}}}{\partial \theta_k} = -\alpha_c e^{-\alpha_c d^{\{p_j\times t\}}}\frac{\partial d^{\{p_j\times t\}}}{\partial \theta_k}\,. \tag{1.17}$$

For $\theta_k = x^{\{t\}}$, (same for $y^{\{t\}}$)

$$\frac{\partial C_i^{\{p\times t\}}}{\partial x^{\{t\}}} = \frac{\alpha_c\left(x^{\{p\}} - x^{\{t\}}\right)}{d^{\{p_j\times t\}}}\rho_i^{\{p_j\times t\}}\,. \tag{1.18}$$

For the derivatives of the mean value we have

$$\begin{aligned}\frac{\partial \mu(\theta)}{\partial \theta_k} =& -10\alpha\frac{\partial \log_{10}\left(d_i^{\{t\}}\right)}{\partial \theta_k} - \frac{\partial C_i^{\{p\times t\}^T}}{\partial \theta_k} C_i^{\{p\}^{-1}} \\ &\left(P_T \mathbf{1}_M - 10\alpha\log_{10}\left(d_i^{\{p\}} - \mathbf{r}_i^{\{p\}}\right)\right)\,.\end{aligned} \tag{1.19}$$

We are now able to compute the CRLB (inverse of the Fisher information matrix) for given prior and current networks. To assess performance of a stochastic current network under a stochastic prior network, a semi-analytic approach is adopted.

Performance Assessment

The adopted approach averages over the random positions of both stochastic networks. This will be followed both without a prior network (sub-section A) as well as with (sub-section B).

1 Performance without CM

For the current network, under no preference for the source position, we place the latter in the middle of a square and model the random positions of the sensors. One such possibility is a two-dimensional Gaussian r.v. The means of all sensor positions will form a square grid of points based on the target density, and variance relative to that density. In all simulations we will assume that the transmitter lies at the center of this deployment, and the sensors capable of measuring its power are determined by a coverage area, a circle around the emitter. The radius of this coverage area is determined by the receive power sensitivity of the measurement network, the transmit power of the emitter, and the propagation characteristics (path-loss exponent).

The simulation process always begins with a very dense realization and gradually we expand the distances of the sensors until the point where less than three sensors are within the coverage area (we have three degrees of freedom (x, y, P), so we need at least three equations). The performance is measured for each step, averaged over different realizations.

Two different propagation scenarios will be examined, one called 'Indoor' and the other 'Outdoor', using respectively a parameterization that tries to reflect such scenarios, i.e. small coverage, de-correlation distance, large path-loss exponent for the indoor scenario and the opposite for the outdoor. The exact values used for those two scenarios are depicted in Table 1.1.

Table 1.1: Parameterization of the propagation scenarios

Parameters	**Scenarios**	
	Indor	Outdoor
Path loss	2	3
Shadow-fading	8	8
correlation coefficient (d_c)	2 ($0.5m$)	0.1 ($10m$)
Range (coverage)	$30dB$ ($3000m^2$)	$80dB$ ($0.6km^2$)

The semi-analytic performance assessment for these two scenarios is conducted by the following way. For a given density of deployment network random realizations of such networks are first produced, and then, based on the coverage, the active sensors are selected. Based only on the active sensors, the CRLB is computed, and averaged over a large number of network realizations. The results for the indoor scenario and for different levels of shadow-fading variance (2 to 16) are depicted in Fig. 1.1. The root mean square error (RMSE) is kept below 1 meter in most cases for a density of 1 sensor per 10 square meters, which is considered very dense. For the case of 1 sensor per $100m^2$, which is a rather sparse for indoor network, the error is bellow $4m$, a value that has been measured experimentally by our group in several measurement campaigns [68]. The coverage area of this example is $33m$, so a $4m$ RMSE is consider unacceptable.

For very sparse networks the shadow-fading plays very important role, and only for very small values localization can be feasible.

For the outdoor scenario, the respective assessment is depicted in Fig. 1.2. The coverage radius in this scenario is 464 meters. The RMSE is small (bellow $6m$) for a rather high density network of 1 sensor per $1000m^2$ and bellow $20m$ for 1 per $10000m^2$. It is clear from the performance results depicted so far that the RSS-based localization for CR applications requires very high density sensor networks, if no CM are utilized.

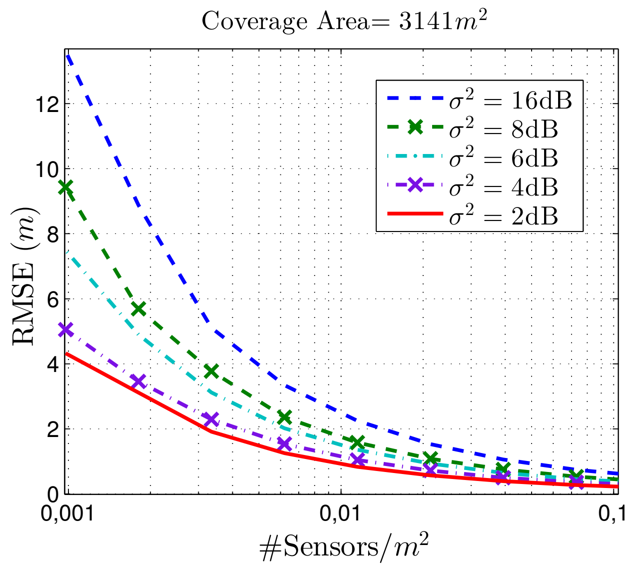

Figure 1.1: Indoor scenario for different shadow-fading values

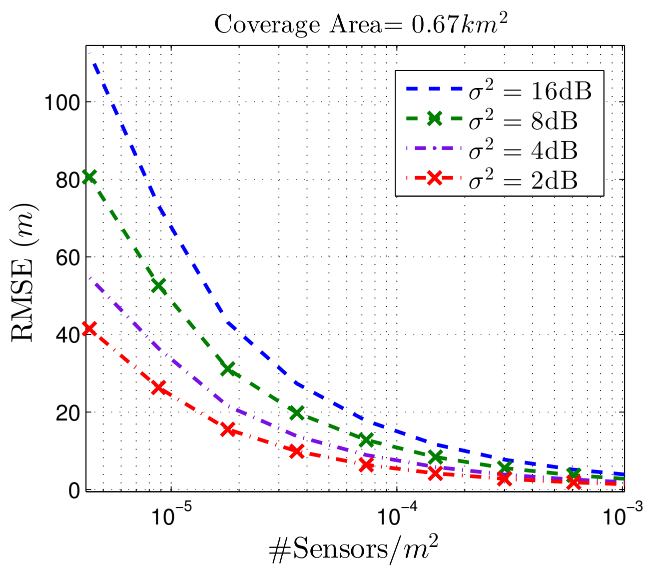

Figure 1.2: Outdoor scenario for different shadow-fading values

2 Performance using CM

This is the most important part of our contribution, since we will examine how the CM can reduce the error and/or the density of the needed measurement network. The process is the same as in the previous section, but here we also have to average out the random positions of the CM. There exist many spatial models used for the positions of radios leading to different performances. Here we model the position of the CM as a homogenous Poisson Point Process (PPP) of a given density λ. The underline pilot density λ is the expected number of points (CM) of the process per unit area (one square meter for indoor and one thousand for outdoor scenario). The case without CM is also depicted ($\lambda = 0$). Starting from the 'indoor' scenario, the performance curves for various densities are provided. Fig. 1.3 depicts the case of indoor scenario (correlation distance of $0.5m$). Theory suggests huge improvement when having dense measurements. For the case of $\lambda = 5$, i.e. the density of the PPP process is 5 sensors per square meter the error is negligible even for very sparse sensor networks. The performance gain is negligible when the density falls below 1 measurement per $10m^2$. As we can see, the expected theoretical gain is huge; enough to enable practical use of RSS-based localization, as long as a dense measurement database of CM is available.

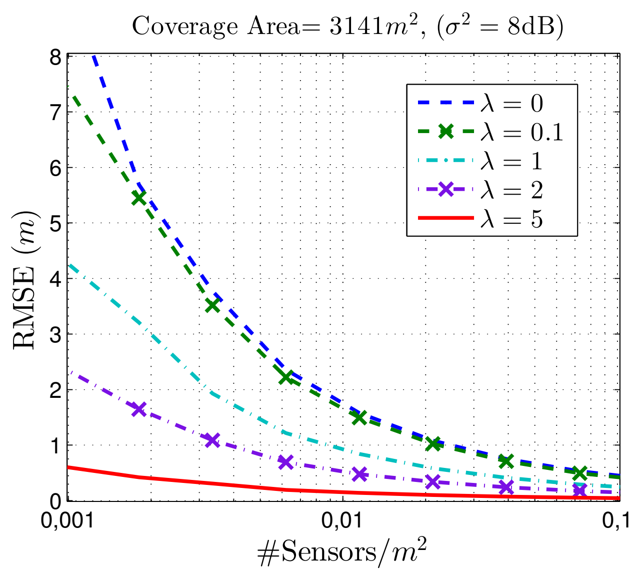

Figure 1.3: Indoor scenario for various pilot placement cases and shadow-fading equal to 8dB

The performance for the 'outdoor' scenario is also depicted in Fig. 1.4.

Equivalent performance enhancement is displayed. When the density is higher than 1 per $100m^2$ the RMSE is bellow $10m^2$ even for very sparse sensor networks. The performance gain is negligible when the density falls below 1 per $1000m^2$.

What we can see is that in theory, the potential of performance enhancement is large when having access to CM with density at the order of the de-correlation distance. What the theory does not say, is the method of getting such performance. The CRLB characterizes the performance of the ML estimator, which is a non-convex optimization problem.

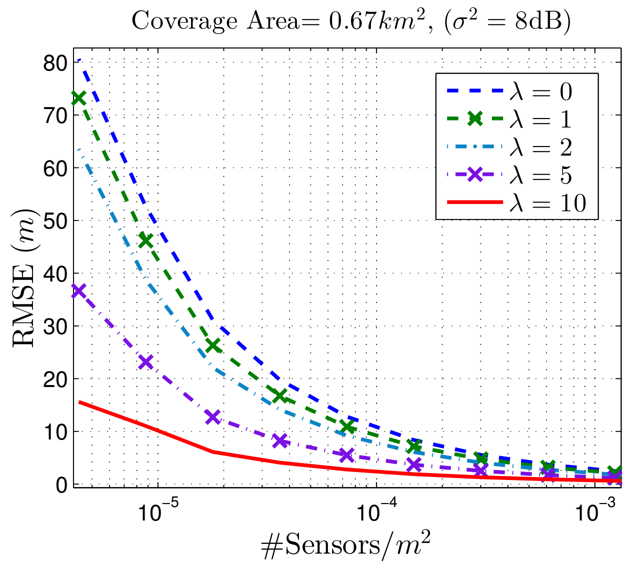

Figure 1.4: Outdoor scenario for various pilot placement cases and shadow-fading equal to 8dB

Conclusions

In this chapter we have provided an assessment of the required network density of sensors for RSS-based localization utilizing CM in a log-normal environment with spatial correlation. We derive the CRLB for the aforementioned case and examine two different scenarios: the first represents the indoor environment and the second the outdoor.

First, we examined the performance without spatial-correlation of the shadow-fading component with respect to the shadow-fading variance, and next we examined the performance of some of these shadow-fading values with respect to different values of deceleration distance. The proper semi-analysis (of the expected accuracy with respect to sensor density) shows that large performance gains are expected when the spatial-correlation is exploited by the use of a CM database. The utilization of CM has been used very often in the literature, but a semi-analytical approach that reveals the scaling of the required sensor network and the maximum expected gain is introduced for the first time.

Chapter 2

Multi Source Power-based localization in correlated log-normal-fading

Parts of this chapter included at: Arvanitakis, George; Dagres, Ioannis;Kaltenberger, Florian; Polydoros, Andreas; "*Cramer Rao lower bound for multi-source localization in spatial-correlated environment*" EUCNC 2015, European Conference on Networks and Communications, June 29-July 2, 2015, Paris, France

This chapter provides the modeling approach and some indicative results on the expected performance of received power-based, multiple-source localization in a spatially-correlated log-normal propagation environment. By properly modeling the approximation of the received signal strength, we are able to evaluate the Crammer-Rao Lower Bound (CRLB) given the positions of the sources and sensors. Probabilistic models are used for both the sensor network as well as the multiple sources, and a semi-analytical approach is taken to compute the average performance of the lower bound. The results are indicative of the expected localization accuracy in a multi-source localization scenario when the correlation of the propagation environment is exploited.

Introduction

While the topic of source localization has been addressed extensively, multi-source localization is less popular due to its inherent difficulty. This is because: There is a limited number of scenarios where multiple non-orthogonal sources may overlap in the same band. For multi-source scenario, the amount of requiring sensors should be at least equal to problem's degrees of freedom, thus, for each unknown transmitter, including power estimation, $3N$ sensors are needed (x_i, y_i, P_i) and in order to make our estimation more resilient to noise we have to use even more. Therefore, the cost of a large number of sensors, a condition necessary for accurate localization, has been thus far prohibitive. However, the potential for cognitive-radio applications (even in 5G), the decreasing cost of sensors, and the availability of databases with localized channel strength measurements are changing this picture.

Theoretical accuracy limits are valuable in order to design a localization system. The most common theoretical bound for power-based localization (Received Signal Strength, RSS) localization, is Crammer-Rao Lower Bound (CRLB) which gives closed form expression about the minimum achievable variance of an estimator. There is extensive literature on the CRLB for single in non-correlated and correlated environment [29] ,[10]. Approximate CRLB and localization algorithms for the multi-source problem was derived in [68]. Our work herein addresses the performance evaluation via the Crammer-Rao Lower Bound (CRLB) of multi-source, power-based localization in spatially-correlated log-normal propagation environment.

The rest of the chapter is organized as follows, Section presents propagation model, basic assumptions and generally clarify all necessary components of our model. Section presents only some indicative results of the performance analysis and finally the conclusions.

Our Model

Power measurements are drawn either from a set of sensors. For each set of i-th sensor and j-th transmitter we adopt the classic log-normal propagation model

$$R_{i,j} = P_j - L_0 - 10\alpha log(d_{i,j}/d_0) - n^s_{i,j} - n^f_{i,j} \ , \tag{2.1}$$

where $R_{i,j}$ is the j-th source power, measured by i-th sensor, $d_{i,j} = \|\mathbf{x}_i - \mathbf{s}_j\|$ is their respective distance ($\mathbf{x}_i$,$\mathbf{s}_j$ are the coordinates of i-th sensor and j-th source, respectively), P_j is j-th emitter power, d_0 is a reference distance and L_0 is the power loss in that reference distance, α is the path-loss exponent, $n^f_{i,j}$ is the noise due to fast-fading, which is hereby modeled as zero-mean Gaussian (in linear scale) and ($n^s_{i,j}$) is the shadow-fading rv. We follow common practice to assume that the fast-fading component can be averaged out and the shadow-fading follows log-normal distribution: a Gaussian rv in the log domain with zero mean and variance σ_s^2.

The model for the correlation factor of Shadow Fading (autocorrelation) in respect to distance is given in [4] :

$$\rho(\Delta x, \Delta y) = \rho(d) = e^{-\frac{\ln(2)d}{d_c}} \ , \tag{2.2}$$

where d_c is the de-correlation distance, meaning that, is the distance where the correlation of tow variables became 0.5. In respect to the reciprocity of the propagation model, we have two types of correlation. One between different sensors and same transmitter, and one by different transmitters and the same sensor.

Due to the eq.2.1 the receiving power of i-th sensor from j-th source is following log-normal distribution at the linear domain. So, the total received power of i-th sensor is $R_i = \sum_{j=0}^{N} R_{i,j}$, where N is the total number of transmitters. But the sum of log-normal is not trivial and approximation needed. As we mention at previews paragraph the shadow fading is spatially-correlated, so, in order to capture the correlation from transmitters side, we use the correlated approximation for the sum of log-normal [69], which give as again a log-normal distribution with mean and variance eq.2.4

$$\mu_i = \frac{1}{c}\left(\ln\left(\sum_{j=0}^{N} e^{cm_i,j}\right) + \frac{c^2\sigma_i^2}{2} - \frac{c^2\bar{\sigma}^2}{2}\right) \ , \tag{2.3}$$

$$\sigma_i^2 = c^{-2}\ln\left(1+\frac{\sum_{k=1}^{N}\left(e^{c^2\bar{\sigma}^2}-1\right)e^{2cm_{i,k}}+2\sum_{j}^{N-1}\sum_{j+1}^{N}e^{c(m_j+m_k)}\left(e^{\rho_{i,j}^{tx}c^2\bar{\sigma}^2}-1\right)}{\left(\sum_{k=1}^{N}e^{cm_{i,k}}\right)^2}\right). \tag{2.4}$$

where $c=\frac{\ln(10)}{10}$ is a constant which is originated from the transformations between natural and log domains, $\rho_{i,j}^{tx}$ is the correlation factor between i-th and the j-th transmitter and calculated from 2.2.

With given mean and variance for each sensor, the general Fisher Information matrix for Gaussian rv is (see [67]):

$$\begin{aligned}[I(\theta)]_{kl} = &\frac{1}{2}tr\left(\mathbf{C}_s^{-1}(\theta)\frac{\partial\mathbf{C}_s(\theta)}{\partial\theta_k}\mathbf{C}_s^{-1}(\theta)\frac{\partial\mathbf{C}_s(\theta)}{\partial\theta_l}\right)\\ &+\frac{\partial\mu(\theta)^T}{\partial\theta_k}\mathbf{C}_s^{-1}(\theta)\frac{\partial\mu(\theta)}{\partial\theta_l}\ ,\end{aligned} \tag{2.5}$$

where $tr()$ is the trace of the matrix and with use of σ_i from eq.2.4 and ρ_{ij}^s correlation factor between i-th and the j-th sensor again from eq.2.2 the covariance matrix of sensors

$$C=\begin{pmatrix}\rho_{11}^s\sigma_1\sigma_1 & \cdots & \rho_{1N}^s\sigma_1\sigma_N\\ \vdots & \ddots & \vdots\\ \rho_{N1}^s\sigma_N\sigma_1 & \cdots & \rho_{NN}^s\sigma_N\sigma_N\end{pmatrix}. \tag{2.6}$$

Results

Some indicative performance results are depicted in this section, mainly the results shows how the localization performance is scaling w.r.t parameters of interest (number of unknown sources, number of sensors, de-correlation distance).

Fig. 2.1 depicts the performance degradation on localizing a source when a second one is at close distance as a function of the sensor network density. The performance for a single source is also depicted for comparative reasons. The parameters used are: pathloss equal to 3, de-correlation distance equal to 5m and shadow fading variance equal to 8dB.

Fig. 2.2 depicts how the CRLB scales w.r.t sensors density, for different number of surrounding sources and the same propagation environment. The number of sources is chosen from a poison point process with a given number of sources density, NoS. Otherwise, NoS parameter shows us the average number of sources within the coverage area of a source, i.e. the expected area where a sensor can detect it is presence.

But, how the performance is scaling w.r.t the spatial correlation? We will answer this question at the next subsection.

Critical Point

A very interesting observation is that the performance (CRLB) as a function of de-correlation distance is not monotonic. Other words, there is not unique answer at the following question "does the spatial-correlation of the shadow fading improve localization accuracy?". We

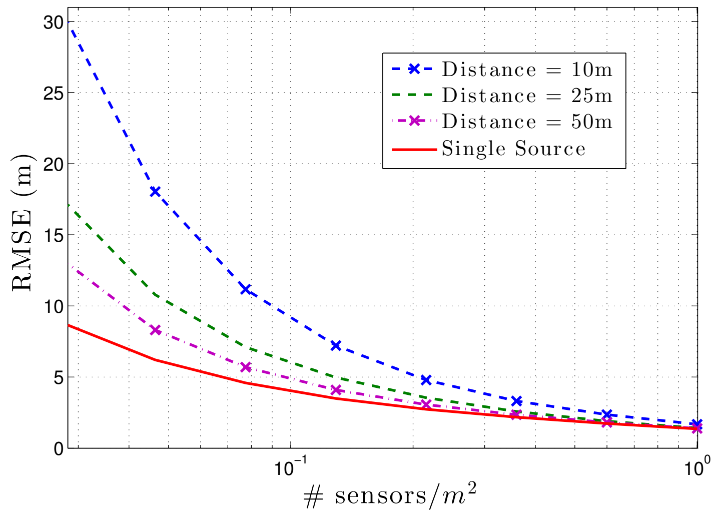

Figure 2.1: Performance by adding second source

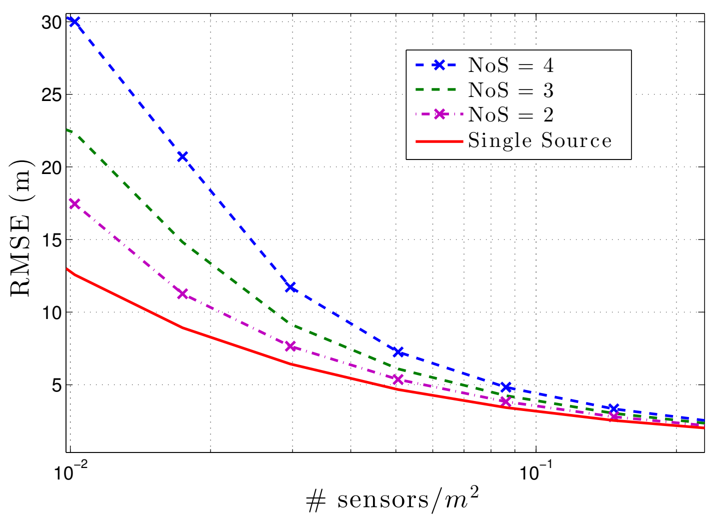

Figure 2.2: Performance for different amount of sources

observed that as the spatial-correlation was raising, the performance was improving until a critical point, after that the performance begun to decrease. We can see it for both single (fig. 2.3) and multiple sources (fig. 2.4). This effect depends heavily on the Geometry of the sensors. In the above cases the source was always in the convex hull of the sensor network.

This behavior can be seen and understood more clear if we focus on a simple example

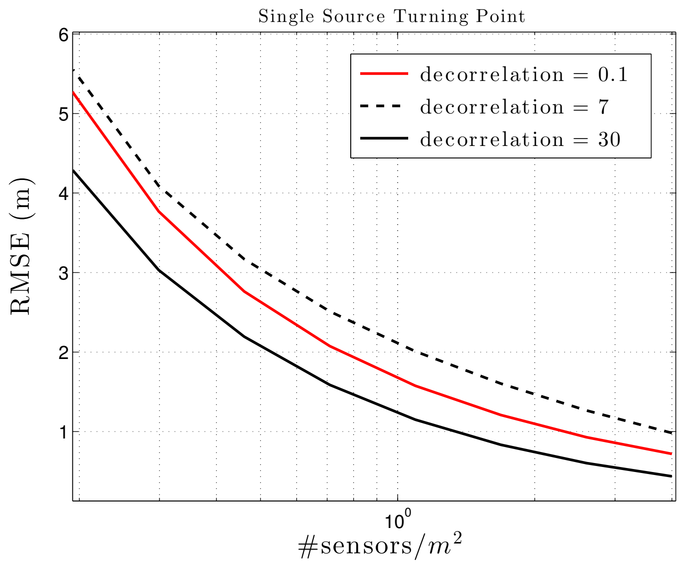

Figure 2.3: Single source performance w.r.t different de-correalation distance

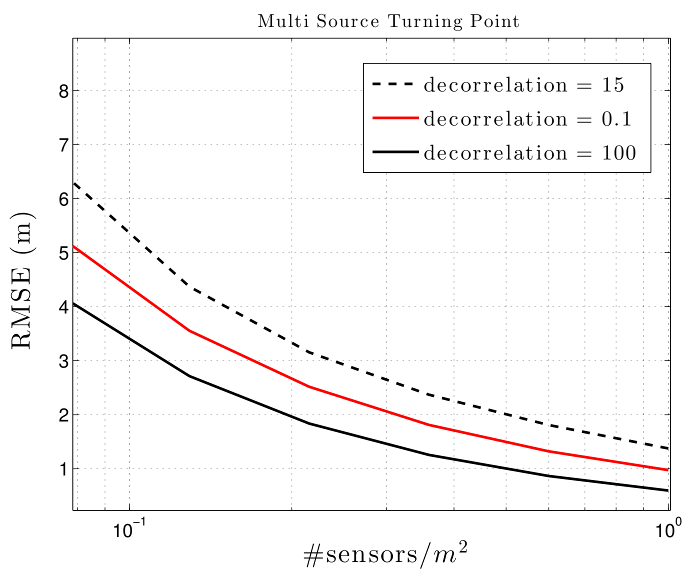

Figure 2.4: Multi source performance w.r.t different de-correalation distance

with one source and two distant piles of sensors fig. 2.5. Red cycle corresponds to CRLB for practically zero de-correlation distance (Environment without spatial-correlation), blue cycle corresponds to de-correlation distance = 2m and black cycle corresponds to de-correlation distance = 10m.

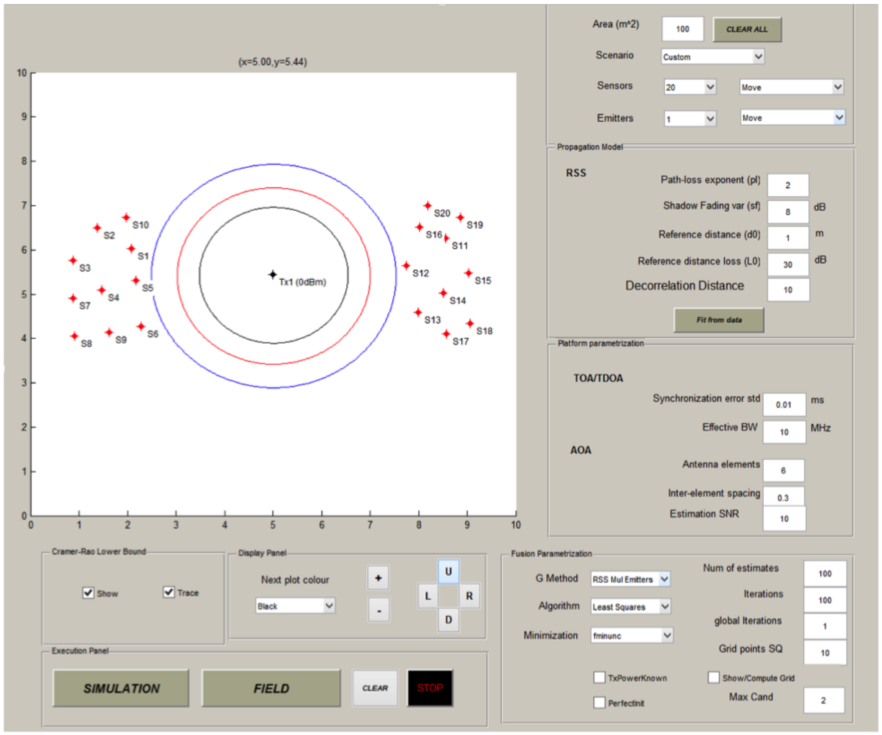

Figure 2.5: A simple example for the critical point

Lets try to explain this phenomenon. Firstly, we assume uncorrelated environment, thats means that each shadow fading component is independent with the others. This shadow fading component adds an error at each pair sensor-source. If the shadow fading component is grater than zero ($n^s > 0$), then the sensor assumes that the source is closer than it is at the reality, if the If the shadow fading component is less than zero ($n^s < 0$), then the sensor assumes that the source is farther than it is at the reality.

As the sources gets more uncorrelated, we can see a performance increase due to the diversity gain. The performance is dropping, as expected, when the correlation increases (we lose diversity). For the extreme case of highly correlated sources (large decorrelation distance, nearly same shadow fading for all sensors), the performance increases again. That is because the propagation model degenerates into a deterministic one (the common error term does not affect the performance). This does not have any practical interest, but it can be very confusing in simulation experiments.

But, as the de-correlation distance is becoming higher, all the sensors will have almost the same shadow fading component, so our system will approaching more and more a deterministic model with just another unknown variable that has to be estimated, the shadow fading variable that will be the same for all the sensors.

Conclusions

This chapter present the initial results of the multi-source scenario in a spatially-correlated environment. First, we set up the multi-source problem and the proper approximations in order to derive the CRLB for this case. Next, we assumed the simplest multi-source scenario, the one with two sources, and we then examined the performance with respect to the distance between the sources. As expected, the performance is inversely proportional to the distance of the sources: if the sources are close enough, the required number of sensors to separate them scales exponentially. Additionally, we showed how the localization accuracy scales with respect to the number of unknown sources and the sensor density. As previously mentioned, the density of sensors in order to achieve a given accuracy scales quadratically with the number of unknown sources.

Finally, we presented an interesting phenomenon on the performance with regards to the de-correlation distance. This strange behavior has not any practical value, but has to be mentioned in order save time from unnecessary debugging time.

Chapter 3

Experimental Campaign I: Characterization of Shadow Fading

The experimental results of an indoor campaign will be presented in this chapter. The measurements of this campaign are very dense in order to capture the statistics of the shadow fading. We are interested in 1) verifying the spatial-correlation of the shadow fading in an indoor environment and 2) obtaining the expected localization accuracy of different ad-hoc techniques as well as identifying practical issues to be further addressed. One main concern is the quantification of scaling on required sensor-network size for achieving a pre-specified localization accuracy.

Experimental Setup

Using semi-analysis we were able to examine how the performance scales without the need to set-up large costly experimental campaigns. How close this view to the reality depends on the modeling assumptions. The simplicity of the adopted model does not allow us to make any strong conclusion. Experimental campaigns are needed to verify, at least, the tendencies. An experimental campaign at an indoor environment is presented herein in order to practically assess the gains of the spatial-correlation.

The set-up was the following: for the sensor network we used one OAI platform, controlling four antennas, each one acting as a different sensor (Rx) located far apart from each other (with lengthy cables). A signal generator was used as a transmitter (Tx) to be localized. The signal generator was tuned at the same central frequency (F_c) with the sensors. Characteristics of Tx and Rx are shown at Table 3.1.

Tx was placed at totally 1846 different positions (grid with step 10cm), blue dots, as we see at Fig. 4.1. Red dots depicts the positions of four Rxs. The total area for this experiment was $\approx 130m^2$. The high density of the measurement campaign covers two purposes. The first one is the need to average out the fast fading. The second one is the need to measure the shadow fading correlation.

Table 3.1: Transmitter / Receiver characteristics

Transmitting signal	Receiver antennas
Random OFDM symbols 0dBm power Isotropic at (x-y) plate Bandwidth = 5 MHz	Fc = 1.9076 GHz Gain = 20dB Isotropic at (x-y) plate

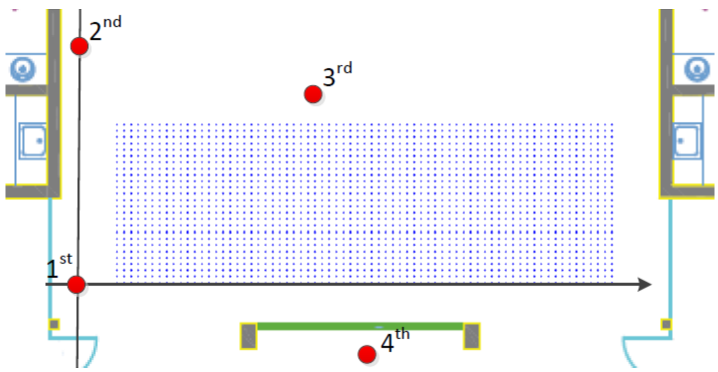

Figure 3.1: Set up of the experimental procedure, red dots indicate the Rxs positions and blue dots the different Tx positions

Post Processing and results

For the fast-fading averaging, we used 9 neighbor points to produce one, like two dimensions moving average. This reduced the grid density, from a $10cm$ step to $30cm$. This $30cm$ is the granularity of our measurement campaign for estimating the spatial-correlation. Having eliminate the fast fading component with the averaging procedure, we estimated the constant parameters of our propagation model eq.2.1 for each sensor. Our estimation criterion is the least-squares and the results are shown at figs. 3.2 - 3.5. So now, easily we can obtain the shadow fading component for each of our emitter positions $n_i^s = P^{tx} - L_0 - 10\alpha log(d_i/d_0) - R_i$.

A different processing procedure was followed in order to visualize this correlation by using a two dimensional moving average filter directly on the dense measurements. The results are depicted in Fig. 3.6 for Rxs 1 & 3, where the parameters of the propagation model were estimated as previous. The correlation can be seen visually. Taking also into account the positions of the Rxs, the existence of angular-correlation is also evident.

Another question that arises regarding the modeling relates to the Gaussianity of the shadow fading. Fig. 3.7 shows the histogram of shadow fading variables for the second Rx and the Gaussian fitting curve. The amount of points is not enough for a smooth result, but the tendency on following a Gaussian distribution can be verified. The model parameters (path-loss, shadow-fading variance) for each Rx is different as opposed to the theoretical modeling assumptions where it was consider the same.

As next step we calculate the de-correlation distance of the environment. At Fig. 3.8 we depict the estimated correlation with respect to distance for all Rxs. The average de-

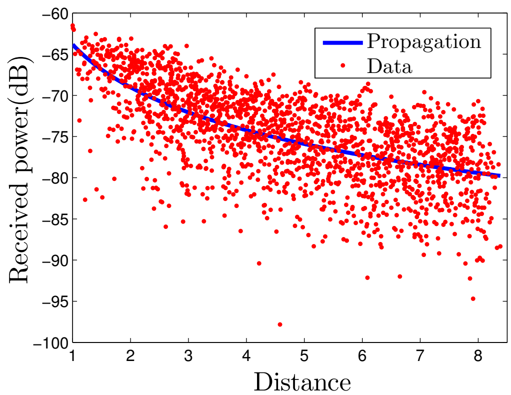

Figure 3.2: Data and estimated propagation model for sensor 1

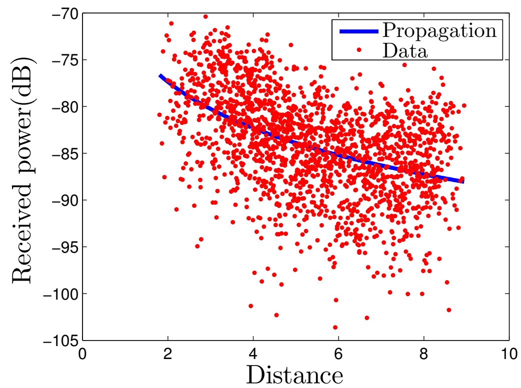

Figure 3.3: Data and estimated propagation model for sensor 2

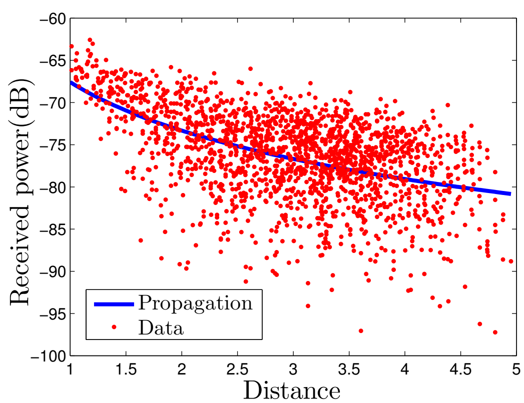

Figure 3.4: Data and estimated propagation model for sensor 3

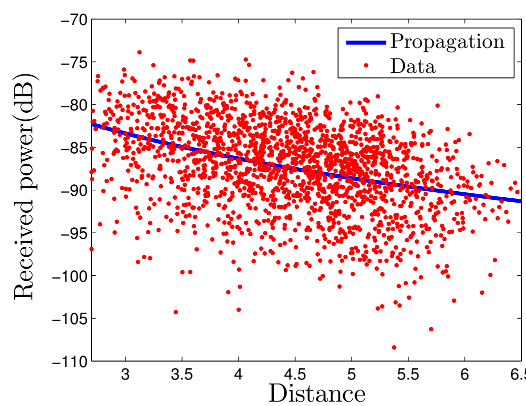

Figure 3.5: Data and estimated propagation model for sensor 4

correlation distance is $d_c \approx 0.65m$.The minimum de-correlation value is $\approx 0.3m$, observed, as expected, for the non-line of sight Rx ($\#4$). We should mention that without the fast-fading averaging, the de-correlation distance is less than $7cm$.

Lastly: what is the performance gain when exploiting CM. We follow an assessment based on the CRLB. More specifically a slight modification of it to support the different propagation parameters per sensor (another deviation from the theoretical model). The key parameter in this assessment is the estimated shadow fading variance (per sensor). Without the CM the shadow fading is modeled as zero-mean. This is not the case with CM.

Using various interpolation techniques (for a given set of CM) we estimate the mean, and then the shadow fading variance that best describes the measurements. The interpolation techniques used for this scope are three deterministic (Linear, Voronoi regions, and Weighted Voronoi [70]) and one probabilistic (Kriging [70]).

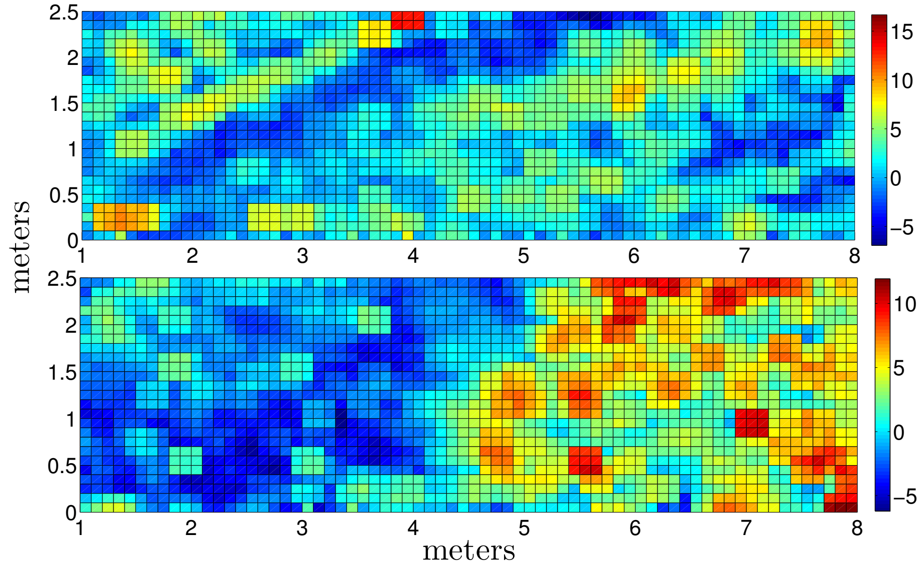

Figure 3.6: Shadow Fading for Rx1 (up) and Rx3 (down)

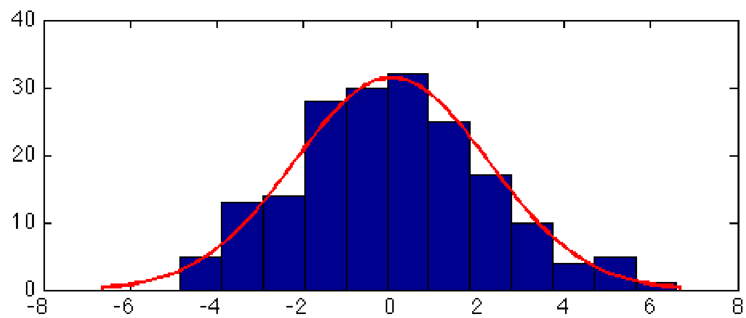

Figure 3.7: Histogram of Shadow Fading

In theory, we choose PPP to model the random position of the CM. Here, we can simulate the probabilistic nature of the CM positions by taking randomly a given portion of the measurements and use them as CM. The process for computing the CRLB of each point depicted in Fig. 4.9 is the following: For the given percentage X (x-axis) and for each point P, we randomly choose $X\%$ of the measurements (also excluding the measurement on point P). Using these measurements as CM the new mean of the shadow-fading of point P is estimated (by spatial interpolation), and by this the new shadow-fading error term. This process is repeated many times and for each point P. By this process we are able to estimate the new shadow fading variance, for each choice of interpolation method, and for the given CM density.

Fig. 4.9 depicts the CRLB (Mean Square Error, MSE) for a reference point at the center of the room, as a function of $X\%$. As expected, the probabilistic interpolation (Kriging)

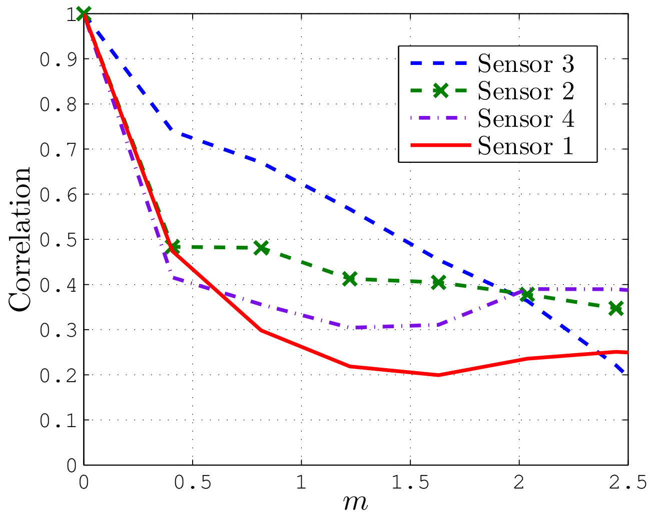

Figure 3.8: Correlation wrt distance

method gives the best performance, which is gradually converges to the case with no CM. The linear interpolation method provide better performance only for dense CM. The Voronoi methods on the other hands provide a good trade-off between performance and complexity.

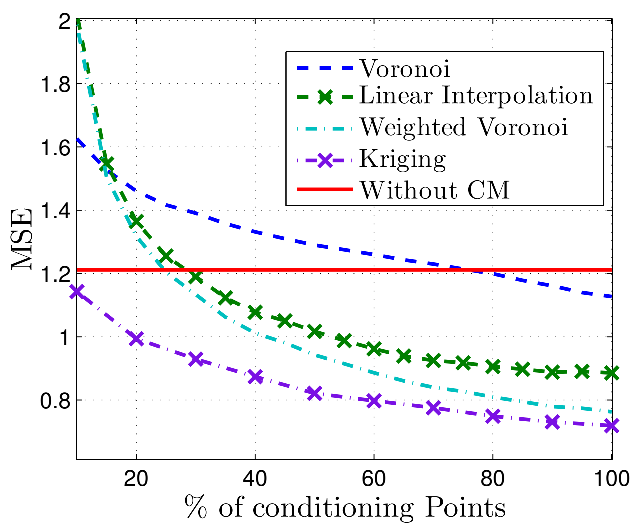

Figure 3.9: Variance for each Interpolation Method

As a final comment, we can say that in practice, for indoor environments, same performance gain is verified. Due to the small de-correlation distance, the density of our measurements did not allowed as to observe the huge gains promised by theory. This means that for indoor environments extremely dense CM is need it.

Conclusions

This chapter presented the results of an experimental assessment using the OAI platform. Using an indoor environment, we performed dense measurements in order to verify the Gaussianity and the spatial-correlation of the shadow-fading component. After the training of our propagation model, both of previous hypotheses were verified. Additionally, the results showed the existence of an angular-correlation of the shadow-fading variable.

Furthermore, after the verification of the spatial-correlation of the shadow-fading component, we investigated different ad-hoc techniques in order to achieve the maximum gain with respect to the density of the CM. The advantage of utilizing past measurements was exploited and the best performance, independent of CM density, was the probabilistic method named Kriging. As a final comment, the ad-hoc techniques that we used improved the localization performance but not as much as the theoretical expectations.

Chapter 4

Experimental Campaign II: Exploiting the correlation of the reverberant indoor environment

Parts of this chapter included at: Arvanitakis, George; Dagres, Ioannis; Kliks, Adrian; Polydoros, Andreas; "*RSS based localization: Theory and experimentation*" EUCNC 2014, European Conference on Networks and Communications, Special session, From Theory to Practice: Experimental Research Activities in NEWCOM#'s EUWIN Labs, 26 June 2014, Bologna, Italy

The experimental results of an indoor campaign will be presented in this chapter. The measurements of this campaign get placed at a wide indoor area. Our goal is to obtain accuracy gain by processing sparse past measurements with simple ad-Hoc techniques. The semi-analysis is helping us to see the big picture, without the need to set-up large costly experimental campaigns. What we were able to do and present it here is a small experiment at an indoor environment in order to assess the gains of the spatial-correlation.

Experimental Setup

The set-up was the following: for the sensor network we used one OAI platform, controlling four antennas, each one acting as a different sensor (Rx) located far apart from each other (with lengthy cables). A second OAI platform was used as a transmitter (Tx) to be localized. It was placed at totally 18 different positions as we see at Figure 4.1. At each position, we took 5 measurements "around" this position to average out the fast fading. The total area for this experiment was $337.5m^2$

After collecting the measurements, the offline processing procedure was the following: Suppose that we want to localize the transmitter when placed at position Tx_i. As a first step we are using all measurements to estimate the parameters of the propagation channel, except the one from Tx_i. Then, based on this estimated channel we localize the source using the measurements from Tx_i. A direct Maximum likelihood (ML) method is used for the localization in all cases. The localization performance in this small scale experiment

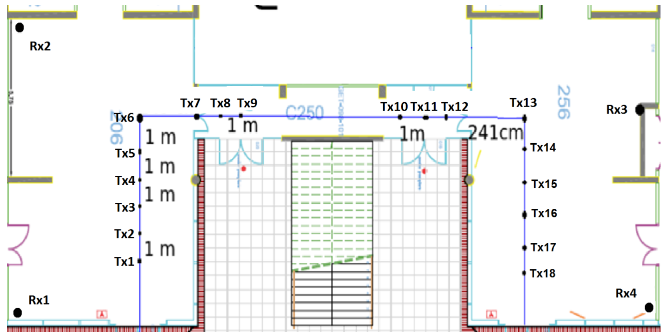

Figure 4.1: Set up of the experimental procedure

is actually a reflection of the suitability of the adopted propagation model. The exact algorithm used for ML is not important.

1 Uncorrelated case

This is the modeling approach, where no spatial-correlation is assumed. The basic parameterization of the log-normal model (2.1) is estimated (through ML) using all other measurements than the one we are interested in (Tx_i). Then based on that model and the measurements from Tx_i we estimate the position. Repeating this procedure for all points, we plot the results in Figure 4.2. We plot with 'x' the estimated position

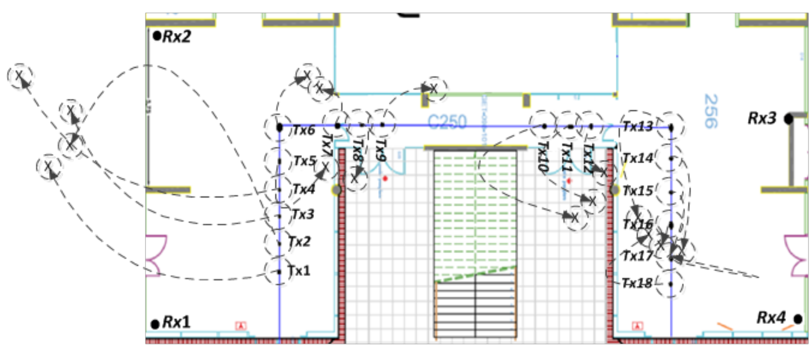

Figure 4.2: Performance results for the Uncorrelated case

2 Correlated Case

In this case we also need to model the spatial-correlation. In the previous sections, we assumed an exponential based spatial-correlation. In reverberant environments, the exponential model does not apply. Various interpolation techniques are used to estimate the shadow-fading field. values that represent your one experimental setup. So, although it is preferred to use the exponential model if you want to describe a large number of experiments in different places, this does not mean that it is the best model to use for a specific setup. In such case, it is best to try estimating directly the shadow-fading field values. Two different approaches will be followed to estimate the shadow fading field, one simplistic based on Voronoi-sets, and one complex, based on interpolation.

Voronoi-set approach: In this simple approach, for each point in space we use the closest pilot to describe the shadow fading field. So, the algorithm that searches for the ML position is also searching for the closest measurement to model the shadow fading. A grid approach is followed for this search. The results from this procedure are displayed in Figure 4.3.

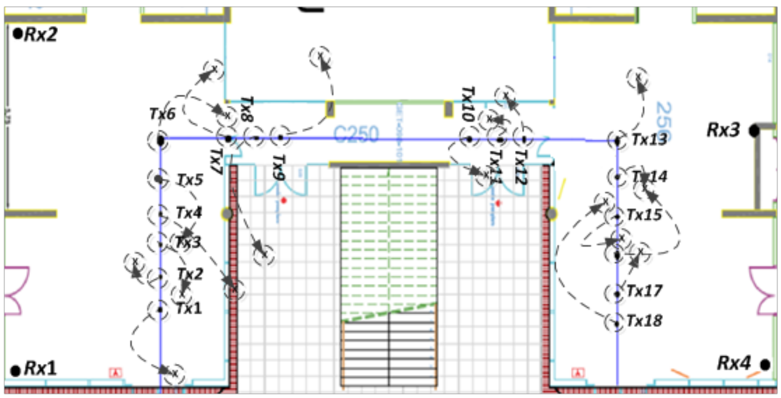

Figure 4.3: Voronoi approach

Interpolation approach: In this approach we are using some selected base functions to model the shadow fading field. Using a trial and error approach and some common sense, we end up dividing the area of interest in different sub-areas as we see in Figure 4.4.

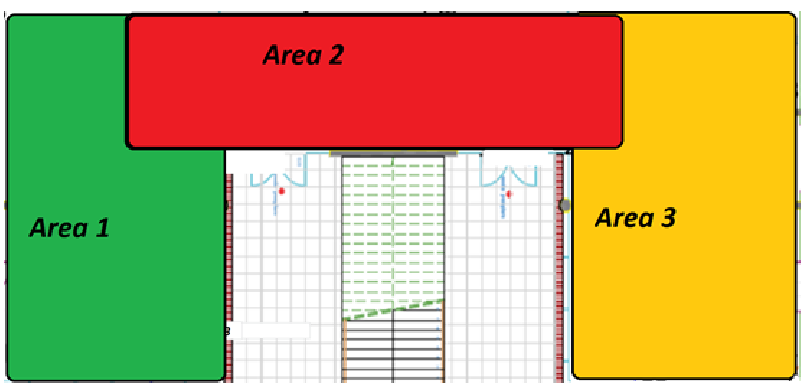

Figure 4.4: Sub-area division

Different interpolation function is used for each region (and for each antenna). Inside of each area we are using only the pilots lying in that area. One dimensional constant, linear and Quadratic interpolation functions are used herein, representing choices of low, medium and high degree of freedom respectively. The straight line orientation of the measurements for each region enforced us to use these simple $1D$ interpolation functions for representing the $2D$ field, by assuming independence from the other dimension. As an example of the fitting we present at Figures 4.5 - 4.8 the results of the different interpolation options for the Area 1 and the four antennas.

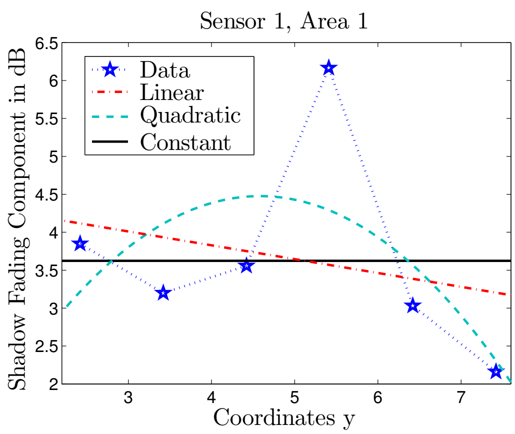

Figure 4.5: Fitting results of Area 1 sensor 1

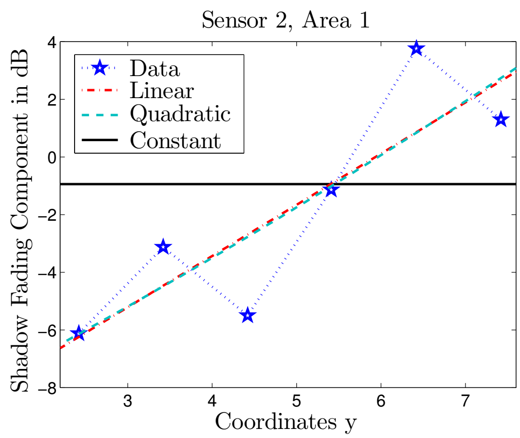

Figure 4.6: Fitting results of Area 1 sensor 2

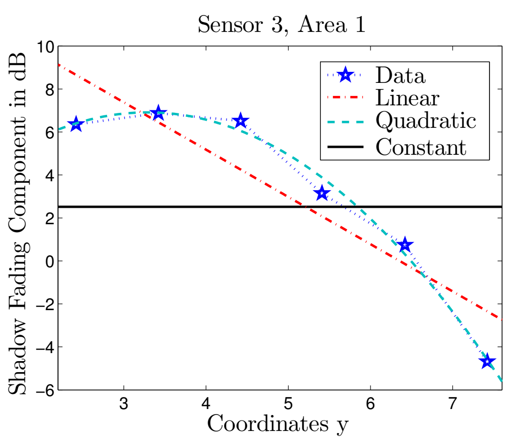

Figure 4.7: Fitting results of Area 1 sensor 3

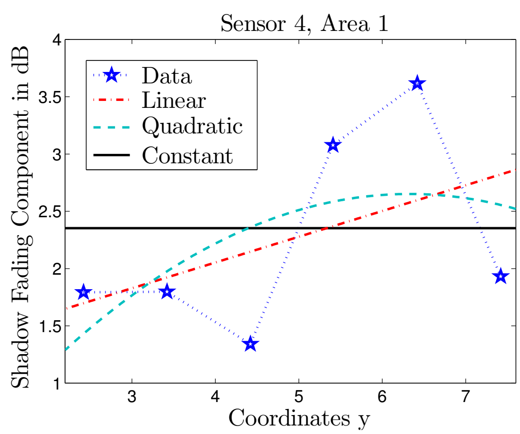

Figure 4.8: Fitting results of Area 1 sensor 4

The blue dot lines represent the measured shadow fading, the red is the linear interpolation and the green the quadratic. We also display the zero-order interpolation.

For the computation of the interpolation parameters again all measurements except from the point of interest are used each time. The term past measurements, used throughout this work does not represent literally this procedure, but that was just a convenient description for systems that store past measurements. The results from using the linear interpolation are displayed in Figure 4.9.

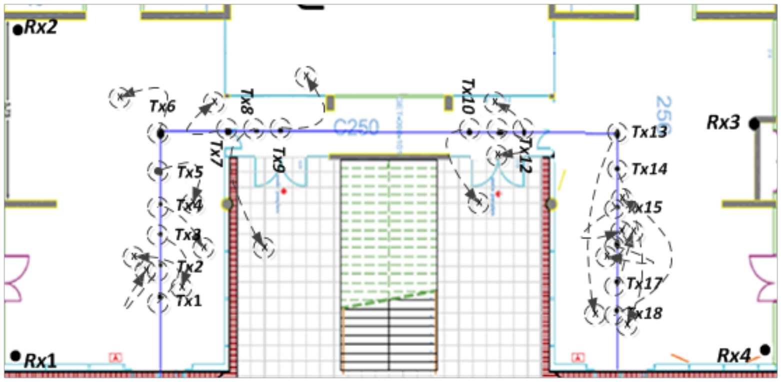

Figure 4.9: Linear Interpolation

The mean square error for all models is displayed in Table 4.1. It is clear, that the use of past measurements improves the performance. The constant interpolation, although better than the uncorrelated case, does not give the best performance, possibly due to under-fitting. The simple Voronoi approach, provides a fairly good performance in comparison with the two other interpolation methods (Linear and Quadratic). Lastly, we see that the Quadratic model gives worse results than the Linear, something that could be accounted to overfitting.

Table 4.1: Mean Error for All Models

	Uncorrelated log-normal	Constant inter-polation	Linear inter-polation	Quadratic inter-polation	Voronoi
All points	4.16	2.95	2.02	2.55	2.15
Excluding 1 worst	3.6	2.68	1.8	2	2.06
Excluding 2 worst	3.1	2.48	1.64	1.88	1.97

Conclusions

In this chapter we have provided an assessment of the required network density of sensors for RSS-based localization utilizing past measurements in a log-normal environment with spatial-correlation. Also presented are the results of another experimental assessment using the OAI platform, focusing on the practical utilization of the spatial shadow-fading correlation.

During this campaign we had very sparse conditioning measurements of a large area, and therefore simple ad-hoc techniques were used to estimate the shadow-fading component of interest by using CM and thereafter applying the maximum likelihood estimator in order to locate the unknown source. This increase in performance by the use of CM is noticeable but not as much as in theory.

Chapter 5

Conclusions & Future Work

In this work, we investigated the spatial-correlation of the shadow-fading. First, we derived the new CRLB for the single-source problem, assuming correlated log-normal fading and knowledge of past measurements. These theoretical results were very promising regarding correlation gain. Next, we provided the CRLB for the multi-source problem in a correlated log-normal environment, but this time without knowledge of past measurements. Our results show that there is not a clear-cut answer to the question, if the correlation of the shadow-fading by itself improves the localization performance. The performance is dropping when the correlation increases, until a critical point where for highly correlated sources (large the performance increases again, because the propagation model degenerates into a deterministic one. The topology of sensors and sources defines the specific value of the critical point.

Additionally, in this master's thesis we performed two experimental campaigns. In the first, we verified the spatial-correlation of the shadow fading in an indoor environment and obtained the expected localization accuracy of different ad-hoc techniques. In the second we estimated the shadow-fading component with different types of ad-hoc techniques and subsequently applied the ML estimator in order to capture the gain of the correlated environment and the CM. In both campaigns, we achieved some gain from the spatial-correlation of the environment but not as much as predicted by the theory.

Currently, we continue our work by investigating the theoretical bounds of the multi-source problem with CM. In addition, methods of verifying the adoption of the approximate sum-log model are under investigation. In terms of the algorithms, we should expand the existing steepest-decent algorithms to use the CRLB in order to converge faster. Except the convergence speed, we should also investigate if we can improve the performance of minimization algorithms by using CRLB in order to get stuck less on local minima. One of the most important issues of localization algorithms.

Indoor localization has got a lot of attention in the last five years. Big tech players such as Google, Apple and Nokia, are in a race to acquire the right technology in order to provide a seamless indoor localization experience just like GPS in outdoor environment. Hundreds of SME's providing different solutions exists.

The technology used for ranging include:

- Various protocols like WiFi, BLE, 802.4.15 (via ToA, TDOA, RSS, AoA)
- Inertial Measurement Units (IMU),(like Accelerometer, Gyro, Compass)
- Ultrasound (via ToA, TDOA)
- Magnetic resonators
- Custom RF (via TOA with Ultra Wideband pulses, or via Phase offset measurements)
- Signals of opportunity (e.g. FM, DVB)
- LEDs (Visible Light Communication)
- Micro-Electro-Mechanical Systems (MEMS)
- Video Camera!

In our work, we focused only on RSS ranging. A future goal is to extend the theoretical performance analysis on ranging techniques that incorporates other technologies too, like the ones mentioned above.

The provided solutions so far uses different mixtures of those technologies. The need for a good Performance Evaluation platform was identified in 2012 Evarilos (FP7, Evaluation of RF-based Indoor Localization, http://www.evarilos.eu/). Microsoft continued this effort (2014, 2015) by issuing an open competition of different solutions. In 2015 23 solutions were evaluated (out of 48 abstract submissions). The outcome, as reported in [71] was:

The Indoor Location Problem is NOT Solved!

- There does not seem to exist a technology or a combination of technologies that can recreate the experience that GPS offers outdoors in the indoor environment
- Applications require much higher granularity of location information for solutions based on WiFi Aps
- There does not seem to be a technology that can consistently provide the same localization error across all evaluation points
- All systems exhibited large accuracy variations across different evaluation points which raises concerns about the stability/reliability of current indoor location technologies.
- Deployment Overhead Remains High
- Changes in the Environment Impact Accuracy

The performance characterization of localization techniques plays a significant role as we continue not to have a clear technology winner. Research projects as Evarilos and private sector initiatives as [71] are one way to go, but, an accompany effort on the theoretical front is equally important. The main problem in such effort is the modeling aspect. In our work a simplistic log-normal model is adopted. There exist various efforts in the literature that tries to accurately model the RSS in indoor environments using some basic geometrical characteristics of the rooms. The extension of our work using more elaborate modeling options is also one of our future goals

Bibliography

[1] J. Mitola, “Cognitive radio - an integrated agent architecture for software defined radio,” *Royal Institute of Technology (KTH)*, may 2000.

[2] P. Casadevall *et al.*, “Radio environmental maps: information models and reference model. document number d4.1,” 2012.

[3] D. Denkovski, V. Rakovic, M. Pavloski, K. Chomu, V. Atanasovski, and L. Gavrilovska, “Integration of heterogeneous spectrum sensing devices towards accurate rem construction,” in *Wireless Communications and Networking Conference (WCNC), 2012 IEEE*, April 2012, pp. 798–802.

[4] M. Gudmundson, “Correlation model for shadow fading in mobile radio systems,” *Electronics Letters*, vol. 27, no. 23, pp. 2145–2146, Nov 1991.

[5] N.-R. Jeon, K.-H. Kim, J.-H. Choi, and S.-C. Kim, “A spatial correlation model for shadow fading in indoor multipath propagation,” in *Vehicular Technology Conference Fall (VTC 2010-Fall), 2010 IEEE 72nd*, Sept 2010, pp. 1–6.

[6] C. Oestges, N. Czink, B. Bandemer, P. Castiglione, F. Kaltenberger, and A. Paulraj, “Experimental characterization and modeling of outdoor-to-indoor and indoor-to-indoor distributed channels,” *Vehicular Technology, IEEE Transactions on*, vol. 59, no. 5, pp. 2253–2265, Jun 2010.

[7] M. Bshara, U. Orguner, F. Gustafsson, and L. Van Biesen, “Fingerprinting localization in wireless networks based on received-signal-strength measurements: A case study on wimax networks,” *Vehicular Technology, IEEE Transactions on*, vol. 59, no. 1, pp. 283–294, Jan 2010.

[8] D. B. Maja Stella, Mladen Russo, “Rf localization in indoor environment,” vol. 21, no. 2, pp. 557–567, June 2012.

[9] R. Vaghefi and R. Buehrer, “Received signal strength-based sensor localization in spatially correlated shadowing,” in *Acoustics, Speech and Signal Processing (ICASSP), 2013 IEEE International Conference on*, May 2013, pp. 4076–4080.

[10] L. Mailaender, “Geolocation bounds for received signal strength (rss) in correlated shadow fading,” in *Vehicular Technology Conference (VTC Fall), 2011 IEEE*, Sept 2011, pp. 1–6.

[11] N. Patwari and P. Agrawal, “Effects of correlated shadowing: Connectivity, localization, and rf tomography,” in *Information Processing in Sensor Networks, 2008. IPSN ’08. International Conference on*, April 2008, pp. 82–93.

[12] *OpenAir Interface, http://www.openairinterface.org/.*

[13] V. Etten, "Navigation systems: Fundamentals of low and very low frequency hyperbolic techniques," *Electr. Commun.*, vol. 45, no. 3, pp. 192–212, 1970.

[14] N. Marchand, "Error distributions of best estimate of position from multiple time difference hyperbolic networks," *Aerospace and Navigational Electronics, IEEE Transactions on*, vol. ANE-11, no. 2, pp. 96–100, June 1964.

[15] H. Lee, "A novel procedure for assessing the accuracy of hyperbolic multilateration systems," *Aerospace and Electronic Systems, IEEE Transactions on*, vol. AES-11, no. 1, pp. 2–15, Jan 1975.

[16] R. Schmidt, "A new approach to geometry of range difference location," *Aerospace and Electronic Systems, IEEE Transactions on*, vol. AES-8, no. 6, pp. 821–835, Nov 1972.

[17] J. M. Delosme, M. Morf, and B. Friedlander, "Estimating source location from time-difference-of-arrival: A linear equation approach," Stanford, Tech. Rep. M355-1, March 1979.

[18] ——, "A linear equation approach to locating sources from time-difference-of-arrival measurements," *IEEE Int. Conf. Acoustics, Speech, and Signal Processing*, pp. 818–824, 1980.

[19] J. O. Smith and J. Abel, "The spherical interpolation method of source localization," *Oceanic Engineering, IEEE Journal of*, vol. 12, no. 1, pp. 246–252, Jan 1987.

[20] B. Friedlander, "A passive localization algorithm and its accuracy analysis," *Oceanic Engineering, IEEE Journal of*, vol. 12, no. 1, pp. 234–245, January 1987.

[21] K. Cheung, H. So, W.-K. Ma, and Y. Chan, "Received signal strength based mobile positioning via constrained weighted least squares," in *Acoustics, Speech, and Signal Processing, 2003. Proceedings. (ICASSP '03). 2003 IEEE International Conference on*, vol. 5, April 2003, pp. V–137–40 vol.5.

[22] K. W. Cheung, H. C. So, W.-K. Ma, and Y. T. Chan, "A constrained least squares approach to mobile positioning: Algorithms and optimality," *EURASIP J. Appl. Signal Process.*, vol. 2006, pp. 150–150, Jan. 2006. [Online]. Available: http://dx.doi.org/10.1155/ASP/2006/20858

[23] K. Ho and M. Sun, "An accurate algebraic closed-form solution for energy-based source localization," *Audio, Speech, and Language Processing, IEEE Transactions on*, vol. 15, no. 8, pp. 2542–2550, Nov 2007.

[24] ——, "Passive source localization using time differences of arrival and gain ratios of arrival," *Signal Processing, IEEE Transactions on*, vol. 56, no. 2, pp. 464–477, Feb 2008.

[25] M. Kazemi, M. Ardebilipour, and N. Noori, "Improved weighted rss positioning algorithm for cognitive radio," in *Signal Processing (ICSP), 2010 IEEE 10th International Conference on*, Oct 2010, pp. 1502–1506.

[26] H. C. So and L. Lin, "Linear least squares approach for accurate received signal strength based source localization," *Signal Processing, IEEE Transactions on*, vol. 59, no. 8, pp. 4035–4040, Aug 2011.

[27] J. Cota-Ruiz, J.-G. Rosiles, E. Sifuentes, and P. Rivas-Perea, "A low-complexity geometric bilateration method for localization in wireless sensor networks and its comparison with least-squares methods," *Sensors*, vol. 12, no. 12, pp. 839–862, 2012.

[28] D. Blatt and A. Hero, "Energy-based sensor network source localization via projection onto convex sets," *Signal Processing, IEEE Transactions on*, vol. 54, no. 9, pp. 3614–3619, Sept 2006.

[29] N. Patwari, A. Hero, M. Perkins, N. Correal, and R. O'Dea, "Relative location estimation in wireless sensor networks," *Signal Processing, IEEE Transactions on*, vol. 51, no. 8, pp. 2137–2148, Aug 2003.

[30] R. Peng and M. Sichitiu, "Robust, probabilistic, constraint-based localization for wireless sensor networks," in *Sensor and Ad Hoc Communications and Networks, 2005. IEEE SECON 2005. 2005 Second Annual IEEE Communications Society Conference on*, Sept 2005, pp. 541–550.

[31] J. Nelson, M. Hazen, and M. Gupta, "Global optimization for multiple transmitter localization," in *Military Communications Conference, 2006. MILCOM 2006. IEEE*, Oct 2006, pp. 1–7.

[32] D. Ampeliotis and K. Berberidis, "Distributed cancellation-based multiple-source localization for wireless sensor networks," in *Signal Processing Conference, 2007 15th European*, Sept 2007, pp. 1921–1925.

[33] R. Martin and R. Thomas, "Algorithms and bounds for estimating location, directionality, and environmental parameters of primary spectrum users," *Wireless Communications, IEEE Transactions on*, vol. 8, no. 11, pp. 5692–5701, November 2009.

[34] C. Jie, "An improved downhill simplex-genetic multiple-source localization in wireless sensor networks," *J. Comput. Inf. Syst*, vol. 7, no. 11, pp. 4007–4014, 2011.

[35] N. Miliou, A. Moustakas, and A. Polydoros, "Interference source localization and transmit power estimation under log-normal shadowing," in *Signal Processing Conference, 2011 19th European*, Aug 2011, pp. 299–2303.

[36] A. Javanmard and A. Montanari, "Localization from incomplete noisy distance measurements," *Found. Comput. Math*, vol. 13, no. 3, pp. 297–345, 2013.

[37] W. Meng, W. Xiao, L. Xie, and A. Pandharipande, "Diffusion based projection method for distributed source localization in wireless sensor networks," in *Computer Communications Workshops (INFOCOM WKSHPS), 2011 IEEE Conference on*, April 2011, pp. 537–542.

[38] W. Meng, W. Xiao, and L. Xie, "A projection based fully distributed approach for source localization in wireless sensor networks," *Ad Hoc Sens. Wirel. Networks*, vol. 18, no. 1-2, pp. 131–158, 2013.

[39] S. Ibeawuchi, S. Dasgupta, C. Meng, and Z. Ding, "Source localization using a maximum likelihood/semidefinite programming hybrid," in *Sensing Technology, 2008. ICST 2008. 3rd International Conference on*, Nov 2008, pp. 585–588.

[40] C. Meng, Z. Ding, and S. Dasgupta, "A semidefinite programming approach to source localization in wireless sensor networks," *Signal Processing Letters, IEEE*, vol. 15, pp. 253–256, 2008.

[41] G. Wang and K. Yang, "Efficient semidefinite relaxation for energy-based source localization in sensor networks," in *Acoustics, Speech and Signal Processing, 2009. ICASSP 2009. IEEE International Conference on*, April 2009, pp. 2257–2260.

[42] R. Ouyang, A.-S. Wong, and C.-T. Lea, "Received signal strength-based wireless localization via semidefinite programming: Noncooperative and cooperative schemes," *Vehicular Technology, IEEE Transactions on*, vol. 59, no. 3, pp. 1307–1318, March 2010.

[43] R. Vaghefi, M. Gholami, and E. Strom, "Rss-based sensor localization with unknown transmit power," in *Acoustics, Speech and Signal Processing (ICASSP), 2011 IEEE International Conference on*, May 2011, pp. 2480–2483.

[44] R. Vaghefi, M. Gholami, R. Buehrer, and E. Strom, "Cooperative received signal strength-based sensor localization with unknown transmit powers," *Signal Processing, IEEE Transactions on*, vol. 61, no. 6, pp. 1389–1403, March 2013.

[45] A. Dogandzic and P. Amran, "Signal-strength based localization in wireless fading channels," in *Signals, Systems and Computers, 2004. Conference Record of the Thirty-Eighth Asilomar Conference on*, vol. 2, Nov 2004, pp. 2160–2164 Vol.2.

[46] X. Sheng and Y.-H. Hu, "Maximum likelihood multiple-source localization using acoustic energy measurements with wireless sensor networks," *Signal Processing, IEEE Transactions on*, vol. 53, no. 1, pp. 44–53, Jan 2005.

[47] J. Nelson and M. Gupta, "An em technique for multiple transmitter localization," in *Information Sciences and Systems, 2007. CISS '07. 41st Annual Conference on*, March 2007, pp. 610–615.

[48] W. Xiao, W. Meng, C. Wu, Z. Jia, and S. Das, "Energy-based sensor network multiple-source localization via a new em algorithm," in *Control and Decision Conference, 2008. CCDC 2008. Chinese*, July 2008, pp. 5319–5324.

[49] W. Meng, W. Xiao, and L. Xie, "An efficient em algorithm for energy-based multisource localization in wireless sensor networks," *Instrumentation and Measurement, IEEE Transactions on*, vol. 60, no. 3, pp. 1017–1027, March 2011.

[50] J. Nelson, M. Gupta, J. Almodovar, and W. Mortensen, "A quasi em method for estimating multiple transmitter locations," *Signal Processing Letters, IEEE*, vol. 16, no. 5, pp. 354–357, May 2009.

[51] J. Nelson, J. Almodovar, M. Gupta, and W. Mortensen, "Estimating multiple transmitter locations from power measurements at multiple receivers," in *Acoustics, Speech and Signal Processing, 2009. ICASSP 2009. IEEE International Conference on*, April 2009, pp. 2761–2764.

[52] V. Cevher, M. Duarte, and R. Baraniuk, "Distributed target localization via spatial sparsity," in *Signal Processing Conference, 2008 16th European*, Aug 2008, pp. 1–5.

[53] H. Krim, D. Tucker, S. Mallat, and D. Donoho, "On denoising and best signal representation," *Information Theory, IEEE Transactions on*, vol. 45, no. 7, pp. 2225–2238, Nov 1999.

[54] E. T. Hale, W. Yin, and Y. Zhang, "Fixed-point continuation for l1 minimization: Methodology and convergence," *SIAM J. Optim*, vol. 19, no. 3, pp. 1107–1130, 2008.

[55] C. Feng, S. Valaee, and Z. Tan, "Multiple target localization using compressive sensing," in *Global Telecommunications Conference, 2009. GLOBECOM 2009. IEEE*, Nov 2009, pp. 1–6.

[56] S. S. Chen, D. L. Donoho, and M. A. Saunders, "Atomic decomposition by basis pursuit," *SIAM Rev.*, vol. 43, no. 1, pp. 129–159, Jan. 2001. [Online]. Available: http://dx.doi.org/10.1137/S003614450037906X

[57] E. Candes and T. Tao, "The dantzig selector: Statistical estimation when p is much larger than n," *Ann. Stat*, vol. 35, no. 6, pp. 2313–2351, 2007.

[58] G. Mateos, J.-A. Bazerque, and G. B. Giannakis, "Spline-based spectrum cartography for cognitive radios," in *Proceedings of the 43rd Asilomar Conference on Signals, Systems and Computers*, ser. Asilomar'09. Piscataway, NJ, USA: IEEE Press, 2009, pp. 1025–1029. [Online]. Available: http://dl.acm.org/citation.cfm?id=1843565.1843790

[59] Q. Ling, G. Wu, C. Jiang, and Z. Tian, "Joint multi-source localization and environment perception in wireless sensor networks," in *Control and Decision Conference (CCDC), 2010 Chinese*, May 2010, pp. 4110–4113.

[60] D. P. Bertsekas and J. N. Tsitsiklis, "Parallel and distributed computation: numerical methods," *Athena Scientific*, 1997.

[61] Q. Ling and Z. Tian, "A decentralized gauss-seidel approach for in-network sparse signal recovery," in *Information Fusion, 2009. FUSION '09. 12th International Conference on*, July 2009, pp. 380–387.

[62] J. Bazerque and G. Giannakis, "Distributed spectrum sensing for cognitive radio networks by exploiting sparsity," *Signal Processing, IEEE Transactions on*, vol. 58, no. 3, pp. 1847–1862, March 2010.

[63] L. Liu, J.-S. Chong, X.-Q. Wang, and W. Hong, "Adaptive source location estimation based on compressed sensing in wireless sensor networks," *Distrib. Sens. Networks*, pp. 1–15, 2012.

[64] H. Rauhut, K. Schnass, and P. Vandergheynst, "Compressed sensing and redundant dictionaries," *Information Theory, IEEE Transactions on*, vol. 54, no. 5, pp. 2210–2219, May 2008.

[65] E. J. Candès, Y. C. Eldar, D. Needell, and P. Randall, "Compressed sensing with coherent and redundant dictionaries," *Applied and Computational Harmonic Analysis*, vol. 31, no. 1, pp. 59 – 73, 2011. [Online]. Available: http://www.sciencedirect.com/science/article/pii/S1063520310001156

[66] H. Jamali-Rad, H. Ramezani, and G. Leus, "Sparse multi-target localization using cooperative access points," in *Sensor Array and Multichannel Signal Processing Workshop (SAM), 2012 IEEE 7th*, June 2012, pp. 353–356.

[67] S. Kay, *Fundamentals of Statistical Signal Processing, Volume I: Estimation Theory*, 1993.

[68] I. Dagres, A. Polydoros, D. Denkovski, M. Angjelicinoski, V. Atanasovski, and L. Gavrilovska, "Algorithms and bounds for energy-based multi-source localization in log-normal fading," in *Globecom Workshops (GC Wkshps), 2012 IEEE*, Dec 2012, pp. 410–415.

[69] A. Safak and M. Safak, "Moments of the sum of correlated log-normal random variables," in *Vehicular Technology Conference, 1994 IEEE 44th*, Jun 1994, pp. 140–144 vol.1.

[70] R. Hemsley, "Interpolation on a magnetic field," Tech. Rep., Sept 2009.

[71] D. Lymberopoulos, J. Liu, X. Yang, R. R. Choudhury, V. Handziski, and S. Sen, "A realistic evaluation and comparison of indoor location technologies: Experiences and lessons learned," in *Proceedings of the 14th International Conference on Information Processing in Sensor Networks*, ser. IPSN '15. New York, NY, USA: ACM, 2015, pp. 178–189. [Online]. Available: http://doi.acm.org/10.1145/2737095.2737726